Revision-II

TO THE EDITOR

Dear Associate Editor,
Dear Dr Daniela Famulari,

We like to thank you for your positive feedback and timely response after receiving the revised version of our manuscript. Please, find attached further modifications made to this revised version.

As before, editor comments are highlighted in yellow, author comments and changes made to the manuscript are depicted in blue. Note, all line numbers quoted in the revisions below refer to the "marked-up" PDF version of the manuscript.

Our particular attention was focused on improving the English language of the manuscript, which we hope has now been addressed to a level of satisfaction.

Yours sincerely in the name of all authors

Anne Wecking

REVISIONS

Editor comment:
The paper presents a study on a field application of an injection technique by means of infrared absorption spectroscopy: it focusses on the comparison of such novel application with the standard GC technique, both using static enclosures to measure N2O exchanges from the soil on the field. The scientific methodology used is good, the graphics are clear and all good standard. I think the results presented are useful for the scientific community, especially relevant to monitoring networks for non-CO2 GHG, where the usage of both micromet methods and enclosure methods is required. Some critical points were highlighted by the reviewers: the authors have subsequently provided the requested clarifications, and added specific material in the supplementary section, comments and to the main manuscript that, to my knowledge, address the raised issues. I would personally like to thank the reviewers for the careful revising work, making it easy for me to proceed with the next step without their further intervention.

Author comment: We agree. Thank you to the two referees, and the editor!

Editor comment:
Non-public comments to the Author: Small note: I encourage the authors to revise again the English throughout the text, and add below some language corrections that got my attention.

- L81: correct the English: "the method real-world application…"
  Author comment: The suggested change was applied.
  Changes made: " […] the method real-world application."

- L81-83: rewrite the sentence as the English is not clear.
  Author comment: The content of the sentence was rewritten and clarified as follows:
  Changes made: "Evidence of concept was provided by statistical tests to assess if the injection method would result in F_{N2O_QCL} equivalent to F_{N2O_GC}, these included: 1) orthogonal regression, 2) Bland Altman, and 3) bioequivalence analyses."

- L. 119: "… the main source", singular.
  Author comment: Verb and object were changed to singular.
  Changes made to the manuscript: " […] which is the main source of N_2O […]."

- L198-200: remove "Whereas". Modify after "…measured by GC analysis, however we found…"
  Author comment: The suggested change was applied, and the sentence split-up into two.
  Changes made to the manuscript: "de Klein et al. (2015) recommended the use of quadratic curves models as the standard curve for C_{N2O} standards measured by GC analysis. However, we found […]."

Further changes made to the manuscript can be found in lines…

Manuscript: **15-18, 21, 22, 28, 31, 39, 48, 49, 52-54, 66, 72, 75, 76, 77, 104, 106, 109-111, 123, 127, 147, 149, 150, 153, 156, 158, 159, 160, 164, 167, 187, 189, 192, 199, 201, 202, 213, 216, 231, 239-244, 246, 248, 252, 255, 256, 282, 283, 285, 293, 301, 304, 317, 318, 332-339, 361, 362, 364-368, 372, 374, 382, 398-402, 410-412, 416-425, 456-462, 464-473, 484, 521-524, 528, 530, 532, 533, 536, 538, 539, 541, 542, 547, 548, 571, 577, 579-582, 584-587, 597, 599, 600, 632, 634, 643, 644, 659, 831, 840, 853, 865, 869, 875, 880, 881, 899, 912, 927, 940, 943, 954, 962,** and **963**

Supplementary material: **6, 7, 18-20, 31, 32, 41, 73**

… and address the editor's comment to provide further revision of the English language throughout the text. Adjustments made to the language focused on the use of articles ('a', 'an', 'the'), hyphens ('-') and commas (,). Redundant wording (e.g. 'for the purpose of', 'prior to') was deleted, the precision of the language enhanced, and long sentences broken into shorter sequences.

Please, note that we also re-arranged our references in the running text of the manuscript. The references should now be placed in alphabetical/chronological order. Changes apply to the following lines:

Manuscript: **49, 52-61, 65-67, 70, 73-74, 100, 208, 237, 411, 478,** and **524**

A novel injection technique: using a field-based quantum cascade laser for the analysis of gas samples derived from static chambers

Anne R. Wecking[1*], Vanessa M. Cave[2], Lìyǐn L. Liáng[3], Aaron M. Wall[1], Jiafa Luo[2], David I. Campbell[1], Louis A. Schipper[1*]

[1] School of Science and Environmental Research Institute, The University of Waikato, Private Bag 3105, Hamilton 3240, Aotearoa New Zealand
[2] AgResearch Ruakura, Private Bag 3123, Hamilton 3240, Aotearoa New Zealand
[3] Manaaki Whenua – Landcare Research, Palmerston North 4442, Aotearoa New Zealand

**Correspondence to*: Anne R. Wecking (arw35@students.waikato.ac.nz), Louis A. Schipper (louis.schipper@waikato.ac.nz)

Abstract. The development of fast-response analysers for the measurement of nitrous oxide (N_2O) has resulted in exciting opportunities for new experimental techniques beyond commonly used static chambers and gas chromatography (GC) analysis. For example, quantum cascade laser absorption spectrometers (QCL) are now being used with eddy covariance (EC) or automated chambers. However, using a field-based QCL EC system to also quantify N_2O concentrations in gas samples taken from static chambers has not yet been explored. Gas samples from static chambers are often analysed by GC, a method that requires labour and time-consuming procedures off-site. Here, we developed a novel field-based injection technique that allowed the use of a single QCL for 1) micrometeorological EC, and 2) immediate manual injection of headspace samples taken from static chambers. To test this approach across a range of low to high N_2O concentrations and fluxes, we applied ammonium nitrate (AN) at 0, 300, 600 and 900 kg N ha^{-1} (AN_0, AN_{300}, AN_{600}, AN_{900}) to plots on a pasture soil. After analysis, calculated N_2O fluxes from QCL (F_{N2O_QCL}) were compared with fluxes determined by a standard method, i.e. here laboratory-based GC (F_{N2O_GC}). Subsequently, the comparability of QCL and GC data was tested using orthogonal regression, Bland Altman and bioequivalence statistics. For AN treated plots, mean cumulative N_2O emissions across the seven-day campaign were 0.97 (AN_{300}), 1.26 (AN_{600}) and 2.00 (AN_{900}) kg N_2O-N ha^{-1} for F_{N2O_QCL}, and 0.99 (AN_{300}), 1.31 (AN_{600}) and 2.03 (AN_{900}) kg N_2O-N ha^{-1} for F_{N2O_GC}. These F_{N2O_QCL} and F_{N2O_GC} were highly correlated (r = 0.996, n = 81) based on orthogonal regression, in agreement following the Bland Altman approach (i.e. within ± 1.96 standard deviations of the mean difference) and shown to be for all intents and purposes the same (i.e. equivalent). The F_{N2O_QCL} and F_{N2O_GC} derived under near-zero flux conditions (AN_0) were weakly correlated (r = 0.306, n = 27) and not found to agree or to be equivalent. This was likely caused by the calculation of small, but apparent positive and negative, F_{N2O} when in fact the actual flux was below the detection limit of static chambers. Our study demonstrated 1) that the capability of using one QCL to measure N_2O at different scales, including manual injections, offers a great potential to advance field measurements of N_2O (and other greenhouse gases) in the future; and 2) that suitable statistics have to be adopted when formally assessing the agreement and difference (not only the correlation) between two methods of measurement.

Deleted: commonly
Deleted: that often
Deleted: time
Deleted: ,
Deleted: :
Deleted: ;
Deleted: comparison
Deleted: derived
Deleted: the
Deleted: the
Deleted: seven
Deleted: zero, i.e.

1 Introduction

Accurate measurements of nitrous oxide (N_2O) emissions from agricultural land are crucial to quantify the contribution of the gas's radiative forcing to climate warming (Thompson et al., 2019). Nitrous oxide is a long-lived greenhouse gas with a global warming potential 265-times higher than that of carbon dioxide (CO_2) over 100 years and is the largest contributor to the depletion of stratospheric ozone (Ravishankara et al., 2009; IPCC, 2013). Agricultural activities on intensively managed soils that receive high inputs of reactive nitrogen (N_r), mostly in the form of animal excreta and nitrogen fertiliser, are the main source of anthropogenic N_2O emissions (Reay et al., 2012). Reactive nitrogen facilitates microbial nitrification and denitrification in the soil with N_2O being an intermediate of these processes (Firestone and Davidson, 1989; Butterbach-Bahl et al., 2013). The production of N_2O in soils is controlled by a multitude of environmental and anthropogenic factors, e.g. soil moisture, nitrogen input and overall farm management, which often result in highly variable N_2O fluxes (Flechard et al., 2007; Erisman et al., 2013; Rees et al., 2013). Adequate and precise flux measurements have, therefore, remained challenging (Rapson and Dacres, 2014; Cowan et al., 2020).

To date, the common method for measuring fluxes of N_2O (F_{N2O}) are closed, non-steady-state 'static chambers' (Lundegard, 1927; Hutchinson and Mosier, 1981); a method used for more than 95 % of all field studies (Rochette and Eriksen-Hamel, 2008; Rochette, 2011; Lammirato et al., 2018). Static chambers are relatively cost-efficient and easy to deploy in the field (Velthof et al., 1996; de Klein et al., 2015). Gas samples are extracted from the chamber headspace during an up to 60-minute enclosure and injected into pre-evacuated glass vials (Rochette and Bertrand, 2003; Luo et al., 2007; van der Weerden et al., 2011). Subsequent analysis of the gas samples is commonly conducted off-site, using gas chromatography (GC) (Luo et al., 2008a; Parkin and Venterea, 2010). However, measurements using static chambers are discontinuous and labour-intensive with uncertainties in F_{N2O} caused by alterations made to the soil environment after installation, pressure differences in the chamber headspace during sampling and the assumption of a linear increase/decrease in gas concentration with time (Denmead, 2008; Christiansen et al., 2011; Chadwick et al., 2014). Through time, different guidelines have been proposed to advance the standardisation of static chamber techniques (Rochette, 2011; de Klein et al., 2015; Pavelka et al., 2018); but essentially the basic method has remained unchanged for decades (Hutchinson and Mosier, 1981; Chadwick et al., 2014).

Alternative approaches to the static chamber method include the use of (semi-) automated chambers and micrometeorological techniques that allow F_{N2O} measurements at higher temporal frequency and resolution (Baldocchi, 2014; Rapson and Dacres, 2014; Pavelka et al., 2018). Recent developments in the technology of fast-response analysers have enabled, e.g. tunable diode laser absorption spectrometers, Fourier transform infrared spectrometers, and, in particular, continuous-wave quantum cascade laser absorption spectrometers (QCL) to be coupled to automated chambers (Cowan et al., 2014; Savage et al., 2014; Brümmer et al., 2017) or eddy covariance (EC) systems (Nicolini et al., 2013; Nemitz et al., 2018). Despite these recent advances in analyser technology, our understanding of the micro- and macro-scale processes that lead to the emission of N_2O has yet remained limited. While chamber measurements help to examine the interaction between soil processes and F_{N2O} at point-scale (Luo et al., 2017), EC promotes the understanding of diurnal, seasonal and annual F_{N2O} dynamics at field to ecosystem levels.

Deleted: ,
Deleted: ; Ravishankara et al., 2009
Deleted: ; Firestone and Davidson, 1989
Deleted: emissions
Deleted: Flechard et al., 2007;
Deleted: Cowan et al., 2020;
Deleted: Hutchinson and Mosier, 1981;
Deleted: Lammirato et al., 2018;
Deleted: ; Velthof et al., 1996
Deleted: Rochette and Bertrand, 2003;
Deleted: Chadwick et al., 2014;
Deleted: ; Denmead, 2008
Deleted: ; Rochette, 2011
Deleted: ; Hutchinson and Mosier, 1981
Deleted: ; Rapson and Dacres, 2014
Deleted: Brümmer et al., 2017;
Deleted: ; Nicolini et al., 2013
Deleted:
Deleted: s
Deleted:
Deleted: ecosystem
Deleted: scale

(Liáng et al., 2018; Cowan et al., 2020). Some studies have aligned chamber and EC measurements to determine the full range of processes, that drive F_{N2O} dynamics across these different scales, but still relied on the use of more than one analyser for measuring F_{N2O} (Jones et al., 2011; Tallec et al., 2019; Wecking et al., 2020a).

In this study, we tested whether a single field-deployed QCL could be used for manual injections of gas samples taken from static chambers to allow near-concurrent measurements of chamber N_2O samples alongside continuous EC. Field measurements using a QCL for both these purposes have, to our knowledge, not yet been conducted. Our objective was to examine whether chamber F_{N2O} determined by field-based QCL (F_{N2O_QCL}) were equivalent to F_{N2O} derived from laboratory GC (F_{N2O_GC}). An important component of this comparison was to demonstrate that manual injections into the QCL offer a robust method for the use in field environments. Our analysis, therefore, reached beyond the sole comparison of two analytic devices (QCL and GC) and also discussed the method real-world application. Evidence of concept was provided by statistical tests to assess if the injection method would result in F_{N2O_QCL} equivalent to F_{N2O_GC}, these included: 1) orthogonal regression, 2) Bland Altman, and 3) bioequivalence analyses.

2 Methods

2.1 Study site

This study was conducted at Troughton Farm, a commercially operating 199 ha dairy farm in the Waikato region, 3 km east of Waharoa (37.78°S, 175.80°E, 54 m a.s.l.), North Island, New Zealand. The farm had been under long-term grazing for at least 80 years with micrometeorological measurements using a QCL EC system made since November 2016 (Liáng et al., 2018; Wecking et al., 2020a). Mean annual temperature and precipitation, recorded at a climate station 13 km to the south-west of the farm (1981–2010), were 13.3 °C and 1249 mm, respectively (NIWA, 2018). The experimental site comprised three paddocks (P51, P53, P54) in the north of the farm with each sized about 2.8 ha. Soils were formed in rhyolitic and andesitic volcanic ash and rhyolitic alluvium. The dominant soil type based on the New Zealand soil taxonomy was a Mottled Orthic Allophanic soil (Te Puninga silt loam) (Hewitt, 2010). Plots used for the static chamber measurement of this study were located on P53 around 50 m to the south-west of the EC system. The physical distance between chamber plots and EC tower ensured that the EC footprint did not experience cross-contamination from any chamber F_{N2O} (Wall et al., 2020).

2.2 Experiment design

One intensive field campaign was conducted between 10 and 16 September 2019. The campaign's primary purposes were to 1) manually collect gas samples from static chambers comprising potentially low to high N_2O concentrations (C_{N2O}); 2) analyse these samples on-site using QCL and off-site using GC; 3) quantify and compare resulting C_{N2O} and F_{N2O}. A thorough description of the QCL operating in EC mode has been provided by Liáng et al. (2018) and Wecking et al. (2020a).

Deleted: ; Liáng et al., 2018
Deleted: ly
Deleted: determined by
Deleted: but
Deleted: as well
Deleted: 's
Deleted: An e
Deleted: ,
Deleted: i.e. assessing if the injection method would result in for practical purposes equivalent F_{N2O_GC} and F_{N2O_QCL},
Deleted: :
Deleted: ;
Deleted: .
Deleted: N_2O fluxes
Formatted: Subscript
Deleted: to

2.2.1 Static chamber measurements

The static chamber trial comprised a randomised block design of circular treatment and control plots each of which included three replicates per treatment/control. Ammonium nitrate (AN) fertiliser was used as a treatment and applied at different rates to ensure production of a wide range of low to high C_{N2O} in the chamber headspace for subsequent measurements. The three application rates were 300 (AN_{300}), 600 (AN_{600}) and 900 kg N ha^{-1} (AN_{900}), while the control plots (AN_0) did not receive any AN. The rates of AN applied were to match nitrogen loading commonly found in cattle excreta patches, which is the main source of N_2O in grazed pastures (Selbie et al., 2015). Separate areas adjacent to the twelve chamber plots were established to collect soil samples for laboratory analyses of soil moisture and soil mineral nitrogen (N_{min}). Soil moisture and water-filled pore space (WFPS) were analysed and calculated using the methods described in Wecking et al. (2020a). Soil N_{min} was derived from field-moist soil samples extracted in 2M KCl (Mulvaney, 1996) and measured colourimetrically using a Skalar SAN++ flow analyser (Skalar Analytical B. V., Breda, Netherlands). Both, NH_4^+ and NO_3^-, were expressed in units kg ha^{-1} using a site-specific soil dry bulk density of 0.73 g cm^{-3} (Wecking et al., 2020a).

Chamber measurements were made on the day of treatment application and throughout the following six days with chamber gas samples collected on nine occasions (Table S1). The sampling followed a standardised chamber technique (de Klein et al., 2003; Luo et al., 2008b; de Klein et al., 2015) and was carried out daily at 10 AM (NZDT) (van der Weerden et al., 2013). Additional sampling was also conducted at noon on 12 and 15 September. Before sampling, PVC lids were fitted to water-filled base channels that provided a gas-tight seal over the 10 L headspace of each chamber. Gas samples were taken from this headspace during a 45 min enclosure period at four times – t_0, t_{15}, t_{30} and t_{45} – per chamber (Pavelka et al., 2018). A sampling port served to extract air from the chamber headspace by using a 60 mL plastic syringe (Terumo Corp., Tokyo, Japan). After flushing the syringe three times with air from the chamber headspace, the following procedure was applied to ensure that GC and QCL analyses would receive identical headspace samples: 1) after flushing, 60 mL of sample air was extracted from the chamber headspace; 2) 10 mL of the sample was discarded to flush the syringe needle; 3) 15 mL was transferred into a pre-evacuated, septum-sealed, screw-capped 5.6 mL glass vial (Exetainer, Labco Ltd., High Wycombe, UK); 4) the syringe needle was flushed again by discarding a further 10 mL; 5) a second pre-evacuated glass vial was over-pressurised with 15 mL, and the remainder discarded. The procedure was repeated for each sample resulting in a total of 2 × 432 samples, i.e. two replicated sample batches for subsequent GC (1 × 432 samples) and QCL (1 × 432 samples) analyses. All samples remained in the septum-sealed Exetainers until analysis.

2.2.2 Laboratory gas chromatography

Gas chromatography was conducted on the first sample batch at the New Zealand National Centre for Nitrous Oxide Measurements (NZ-NCNM) at Lincoln University, New Zealand. Automated analysis (GX-271 Liquid Handler, Gilson Inc., Middleton, WI) was performed using a SRI 8610 GC (SRI Instruments, Torrance, CA, USA) and a Shimadzu GC-17a (Shimadzu Corp., Kyoto, Japan) equipped with a ^{63}Ni-electron capture detector. The analysis followed standard procedures

Deleted: flux
Deleted: are
Deleted: s
Deleted: Flux
Deleted:
Deleted: ; Luo et al., 2008b
Deleted: the
Deleted: s
Deleted: i
Deleted: d
Deleted: and

described in detail by de Klein et al. (2015). Oxygen-free, ultra-high purity nitrogen (N_2) was used as the carrier gas (mobile phase) at a flow rate of 0.4 L min^{-1}. The measurement frequency was set to 1 Hz. Sample Exetainers experienced a storage time of up to two weeks before analysis which was due to transportation from the field site to the laboratory. The run time during GC analysis was about eight minutes per sample.

2.2.3 Field quantum cascade laser absorption spectrometry

The second batch of N_2O samples was collectively analysed on the day after the last chamber sampling, 17 September, by manual injection into a continuous-wave quantum cascade laser absorption spectrometer (QCL, Aerodyne Research Inc., Billerica, MA, USA). Briefly, QCL uses infrared (IR) light energy which is passed through a 0.5 L multiple pass absorption cell with a pathlength of 76 m. Inside the cell, N_2O absorbs IR light energy which then is quantified as equivalent to the compositional N_2O concentration of the gas sample measured (Nelson et al., 2004).

For the purpose of our analysis, we switched the QCL from its continuous measurement (EC) mode to an 'injection mode'. The injection mode conversion took less than 30 minutes: a stainless steel three-way valve (Swagelok, Solon, OH, USA) mounted to the air inlet of the QCL allowed re-direction of the airflow from the primary inlet tube of the EC system into a second, 1 m long Bev-A-line tube (4 mm internal diameter). At its end, the tube was connected to a pressure regulator and a bottle of oxygen-free, industrial-grade N_2 carrier gas (BOC Ltd., NZ). Two stainless steel, T-junction connectors (Swagelok, Solon, OH, USA) were fitted to the sample tube allowing the overflow of excess carrier gas through a 0.45 µm PTFE membrane filter (ThermoFisher, Scientific, NZ) and sample injection through a septum-sealed port (Fig. 1). A dry scroll vacuum pump (XDS35i, Edwards, West Sussex, UK) was used for both EC measurements and manual injections to continuously draw either air or carrier gas through the QCL sample cell.

[FIGURE 1 ABOUT HERE]

Once the injection line had been established, the flow rate was reduced from an initial 15 L min^{-1} used for EC to 1 L min^{-1} for manual injections based on Savage et al. (2014), Lebegue et al. (2016) and Brümmer et al. (2017). The reduction in flow was monitored using a RMA-SSV flow meter (Dwyer Instruments, PTY. Ltd., Michigan City, IN, USA) while setting the inlet control valve of the QCL to 2 V (using the TDLWintel software command) before manually adjusting inlet and outlet control valves of the QCL device further until the desired flow rate was achieved. Prior to sample injection, a minimum lag time of ten minutes was applied to let temperature and pressure of the QCL and its temperature-controlled enclosure box return to steady-state, i.e. 35 ± 0.5 Torr, 33.5 °C laser temperature, and a QCL enclosure box temperature of 30 ± 0.1 °C.

Standards of certified N_2O concentration (range 0.2 to 100 ppm) were injected before, during and after each sample run and complemented QCL analysis (Table S2). Ten out of the twelve N_2O standards were provided by the NZ-NCNM (except 0.321 and 0.401 ppm) and, therefore, identical to those used for GC (Sect. 2.2.2). The QCL measurements were made at 10 Hz frequency with 1 mL of sample air extracted from each sample Exetainer and manually injected into the flow of N_2 carrier gas by using a 1 mL glass syringe (SGE International PTY Ltd., VIC, Australia). The glass syringe was flushed with N_2 gas after each injection to avoid cross-contamination of samples and N_2O standards. The selection of syringe type, flow rate and the

Deleted: ultra
Deleted: prior
Deleted: to
Deleted: their
Deleted: collectively
Deleted:
Deleted: oxygen
Deleted: industrial
Deleted: Lebegue et al. (2016),
Deleted: were

usage of N_2O standards were based on preliminary tests conducted in advance of the actual field campaign. Finally, it was important to keep a chronological record of the injected sample sequence to allow for a later re-identification of samples in the raw output data of the QCL.

2.3 Data processing

GC and QCL analyses resulted in the output of peak area data from the injected N_2O standards and chamber derived N_2O samples (Fig. S1). Data processing, therefore, first had to determine the relationship between peak area and (known) N_2O concentration (C_{N2O}) of the injected standards. To compute the final but initially unknown C_{N2O} of chamber N_2O samples, peak area data from N_2O standards were fitted to linear and quadratic (second-order-polynomial) models (van der Laan et al., 2009; de Klein et al., 2015). de Klein et al. (2015) recommended the use of quadratic curves models as the standard curve for C_{N2O} standards measured by GC analysis. However, we found that both linear and quadratic models adequately fitted C_{N2O} standards derived from QCL. Using a linear fit ultimately resulted in, on average, 3 % smaller F_{N2O_QCL} (range -0.5 to -4.3 %) than using a quadratic model. Nonetheless, since the quadratic fit suited lower C_{N2O} better than a linear fit, quadratic models were applied to represent the standard curves from injected standards of known C_{N2O} (Fig. S2). The quadratic model used to calculate final C_{N2O} was based on a selection of standards fitted to the expected minimum and maximum range of real sample C_{N2O}; which in our study ranged between 0.3–10 ppm (Fig. S1, Table S2). Output data from GC were processed in PeakSimple software (SRI Instruments, Torrance, CA, USA) and Excel (Microsoft Corp. Redmond, WA, USA). MATLAB R2017a scripting (MathWorks Inc., Natick, MA, USA) served the processing of data derived from the QCL.

2.4 Flux calculation

The F_{N2O} in mg N_2O-N m^{-2} hr^{-1} was calculated for both data streams, GC (F_{N2O_GC}, n = 108) and QCL (F_{N2O_QCL}, n = 108), by applying a linear regression function to the increase in chamber headspace C_{N2O} between time t_0 and t_{45} following Eq. (1) (van der Weerden et al., 2011):

$$F_{N2O\_GC} \text{ and } F_{N2O\_QCL} = \frac{\Delta N_2O}{\Delta T} \times \frac{M}{Vm} \times \frac{V}{A} \quad (1)$$

where ΔN_2O is the increase in headspace C_{N2O} (µL N_2O L^{-1} (ppmv)) with time; ΔT is the enclosure period (in hours); M is the molar weight of nitrogen in N_2O (44 g mol^{-1}); Vm is the molar volume of gas (L mol^{-1}) at the mean air temperature recorded at each sampling occasion; V is the chamber headspace volume (m^3); and A is the area covered by the chamber base, here 0.0415 m^2. All F_{N2O} were converted to units of nmol N_2O m^{-2} s^{-1} to allow for comparability between GC and QCL outputs. The integration of F_{N2O_GC} (n = 84) and F_{N2O_QCL} (n = 84) measured at 10 AM sampling was used to quantify the proportion of applied nitrogen emitted as N_2O (E_{N2O}) across the seven day trial in units kg N_2O-N ha^{-1} based on Luo et al. (2007) and Wecking et al. (2020a).

Deleted: ; van der Laan et al., 2009
Deleted: Whereas
Deleted: ,
Deleted: %
Deleted: used
Deleted: build
Deleted: actual
Deleted: of the gas samples
Deleted: was
Deleted: was
Deleted: used for
Deleted: N_2O flux
Formatted: Subscript
Deleted: over
Formatted: Not Superscript/ Subscript
Deleted: determined

2.5 Statistical analyses

The statistical analysis for C_{N2O} data (C_{N2O_GC} and C_{N2O_QCL}, each n = 432) and resulting F_{N2O} (F_{N2O_GC} and F_{N2O_QCL}, each n = 108) was conducted in Genstat® (Version 19, VSN International, Hemel Hempstead, UK). After testing for normality using a Shapiro-Wilk test and homogeneity of variance by examining residual and fitted values, we applied three different statistical approaches to compare GC with QCL data: 1) orthogonal regression, 2) Bland Altman and 3) bioequivalence statistics.

The orthogonal regression analysis used standardised C_{N2O} and F_{N2O} data following Eq. (2):

$$standardised\ C_{N2O}\ and\ F_{N2O} = \frac{(x - mean)}{standard\ deviation} \quad (2)$$

The core of this orthogonal regression was a principal component analysis which, in contrast to ordinary least square regression, allowed for measurements errors in the response and the predictor variable by minimising the squared residuals in a vertical and horizontal direction. While orthogonal regression returned a Pearson correlation coefficient r that provided information about the strength of the linear relationship between GC and QCL data, we found that r did not include any prediction about the level of agreement between the two methods (Bland and Altman, 1986; Giavarina, 2015). The degree to which GC and QCL data would agree was, for that reason, determined by using Bland Altman statistics that quantified the bias (i.e. the mean difference) and the limits of agreement between the two methods. The limits of agreement were calculated from the mean and the standard deviation (SD) of the difference between GC and QCL data. We defined that 95 % of all data points had to be within ± 1.96 SD of the mean difference (Giavarina, 2015). The Bland Altman analysis was conducted for individual F_{N2O} as well as for mean F_{N2O} across replicates of the same treatment.

Still, testing for correlation and agreement did not determine whether GC and QCL data would effectively and for practical purposes be the same (termed 'equivalent'). We, therefore, used bioequivalence statistics to assess the biological and analytical relevance of the difference between the two methods. The first part of this analysis comprised a one-way analysis of variance (ANOVA) for F_{N2O} which was subset by treatment (AN_0, AN_{300}, AN_{600}, AN_{900}) and analytical device (GC, QCL). Results from this ANOVA determined the 90 % confidence intervals (CI) of the mean difference between F_{N2O_QCL} and F_{N2O_GC}. In bioequivalence statistics, the 90 % CI (at a standard power level of 80 %) is generally preferred instead of using a 95 % CI that often serves to establish a statistical difference between two methods or treatments rather than proving no difference. An important component of the analysis was to also define the equivalence range, i.e. the maximum acceptable difference, between the new (QCL) and the standard method (GC). Bioequivalence statistics acknowledge that two methods will never be exactly the same. Defining an acceptable equivalence range is, thus, an important precondition and might in some cases be even provided by a regulatory authority. Originating from pharmaceutical research (Bland and Altman, 1986; Giavarina, 2015; Patterson and Jones, 2006; Rani and Pargal, 2004), the concept of bioequivalence has not broadly been applied in environmental sciences. Therefore, an acceptable equivalence range for N_2O data based on the use of different analysers and methods has yet to be defined. We determined that the maximum acceptable difference of F_{N2O_QCL} had to be as small as possible and within ± 5 % of the mean difference of the standard method (F_{N2O_GC}). The null hypothesis (F_{N2O_QCL} is different

Deleted: both

Deleted: a

Deleted: n

Deleted: While commonly used in

Deleted: in our study

from F_{N2O_GC}) was rejected when the 90 % CI of the difference (F_{N2O_QCL}-F_{N2O_GC}) was entirely within the predefined equivalence range at a significance level of 5 %. Following the same principles, we conducted a bioequivalence analysis for C_{N2O_QCL} and C_{N2O_GC}.

3 Results and discussion

3.1 Environmental conditions and soil variables

Daily mean air temperatures during the seven-day chamber campaign ranged from 8.3 to 12.8 °C. The WFPS of the soil within the chambers and associated plots did not fall below 73.9 % with a mean of 79.5 %. The cumulative rainfall in September 2019 was 119 mm of which only 2 mm occurred during the seven days of the campaign. As expected, soil NH_4^+ and NO_3^- levels increased with increasing application of AN fertiliser. The highest values of N_{min} measured at AN_{900} plots were 265 kg NH_4^+ ha^{-1} and 268 kg NO_3^- ha^{-1}. The mean background levels of soil NH_4^+ and NO_3^- were around 2 kg ha^{-1}. At the end of the campaign, soil NH_4^+ levels for all treatments had decreased by less than half while the amount of soil NO_3^- remained similar to the initial level measured on the day of treatment application (Table S3).

3.2 Comparing GC and QCL derived data

3.2.1 Magnitude and general variability

Measurements resulted in a wide range of F_{N2O} but followed the same temporal and treatment-dependent patterns for both F_{N2O_GC} and F_{N2O_QCL}. The magnitude of individual fluxes was between -0.10 and 22.24 nmol N_2O m^{-2} s^{-1} for F_{N2O_GC} and -0.07 and 22.81 nmol N_2O m^{-2} s^{-1} for F_{N2O_QCL}. The mean F_{N2O} (n = 27) from chamber plots that received the highest application rate of AN fertiliser (AN_{900}) was 13.22 nmol N_2O m^{-2} s^{-1} ± 1.47 (± standard error of the mean, SEM) for F_{N2O_GC} and 13.27 nmol N_2O m^{-2} s^{-1} ± 1.43 for F_{N2O_QCL}. Similarly, the AN_{600} treatment had a mean F_{N2O} of 8.51 nmol N_2O m^{-2} s^{-1} ± 0.98 (F_{N2O_GC}) and 8.33 nmol N_2O m^{-2} s^{-1} ± 0.9 (F_{N2O_QCL}). The mean F_{N2O} for AN_{300} was 6.61 nmol N_2O m^{-2} s^{-1} ± 0.78 (F_{N2O_GC}) and 6.48 nmol N_2O m^{-2} s^{-1} ± 0.69 (F_{N2O_QCL}). At control plots, F_{N2O} were close to zero (Fig 2; Table S3). We found that treatment F_{N2O} increased from a near-zero background flux to ≥ 8.5 nmol N_2O m^{-2} s^{-1} on the second day of the campaign. From then, AN_{300} fluxes gradually decreased with time whereas F_{N2O} at AN_{600} and AN_{900} plots remained relatively elevated until the last day of the trial (Fig. 2). These temporal trends aligned with findings from Cowan et al. (2020) who observed N_2O emissions to peak within seven days after urea and AN fertiliser application, and found that F_{N2O} returned to background levels after two or three weeks. Similarly, short-term responses of F_{N2O} to AN application were determined by others, e.g. Bouwman et al. (2002); Jones et al. (2007) and Cardenas et al. (2019). However, for our study, AN treatment effects on F_{N2O} were of secondary interest. Different rates of AN fertiliser were only applied to result in a wide range of C_{N2O} and F_{N2O} (low to high) and thereby, allow to compare GC and QCL data.

[FIGURE 2 ABOUT HERE]

Deleted: C
Deleted: compared
Deleted: to
Deleted: ing
Deleted: near
Deleted: for
Deleted: ;
Deleted: also
Formatted: Subscript
Deleted: and thereby to
Deleted: for
Deleted: a methodological comparison of

3.2.2 AN treatment flux and concentration data

The correlation between calculated F_{N2O_GC} and F_{N2O_QCL} and between C_{N2O_GC} and C_{N2O_QCL} across all treatments was high with an r value of 0.996 resulting from orthogonal regression (Fig. 3a, 3b). For both cases, major axis, ordinary and inverse least squares were nearly identical to a 1:1 line. All three regression models could therefore be used similarly well to predict the strength of the linear relationship between F_{N2O_GC} and F_{N2O_QCL} and C_{N2O_GC} and C_{N2O_QCL}, respectively (Table S4). The results of the orthogonal regression analysis suggested that QCL delivered equivalent data to the GC method. The Bland Altman statistic quantified a percentage difference between the two methods for F_{N2O} (i.e. F_{N2O_GC} and F_{N2O_QCL} treatment means) of not smaller than -11.2 % and not greater than +9.2 % (Table S5). The percentage difference between individual F_{N2O_GC} and F_{N2O_QCL} (not treatment means) was slightly greater but in only less than 3 % of all cases exceeded +10 % and -15 %. This was likely due to the higher variability of F_{N2O} between individual replicates of the same treatment than across calculated means. For both cases, ≥ 95 % of all data points were well within the pre-defined limits of agreement ± 1.96 SD (Fig. 4b). The overall mean difference (bias) between F_{N2O_GC} and F_{N2O_QCL} was 0.1 nmol N_2O m^{-2} s^{-1} (Fig. 4b). However, this small bias might be practically irrelevant when compared with the overall detection limit of static chambers and other method-associated uncertainties. Neftel et al. (2007), for instance, quantified the detection limit of static chambers to be 0.23 nmol N_2O m^{-2} s^{-1}, and Parkin et al. (2012) reported 0.03 nmol N_2O m^{-2} s^{-1}. In contrast, Flechard et al. (2007) and others (e.g. Rochette and Eriksen-Hamel, 2008; Jones et al., 2011) showed that the uncertainty of integrated chamber F_{N2O} can be as high as 50 % at the annual scale.

[FIGURE 3 and 4 ABOUT HERE]

3.2.3 Control flux and concentration data

In contrast to the strong comparability of GC and QCL data at AN treatment sites, F_{N2O_GC} and F_{N2O_QCL} measured at control plots (AN_0) were only poorly correlated (r = 0.3064) (Fig. 3c). The model-fit of the major axis, ordinary and inverse least squares indicated that the regression of F_{N2O_GC} on F_{N2O_QCL} (and vice versa) was not identical, i.e. differed in the minimisation of squared residuals in a vertical and horizontal direction. Likewise, this also applied to C_{N2O_GC} and C_{N2O_QCL} (Fig. 3d). Mean F_{N2O} ranged from a minimum of -0.05 to a maximum of only 0.21 nmol N_2O m^{-2} s^{-1} (Table S3). Consequently, Bland Altman statistics determined only small quantitative differences between F_{N2O_GC} and F_{N2O_QCL}. When computing the percentage difference between these F_{N2O_GC} and F_{N2O_QCL}, we found near-zero F_{N2O} from AN_0 plots were less consistent in relative terms than treatment F_{N2O} (Fig. 4, Table S5). However, these inconsistencies were generally small and did not appear of great biological interest.

More generally, QCL analysis resulted in slightly higher C_{N2O} than GC, which explains why the calculated F_{N2O_QCL} at AN_0 plots were higher than F_{N2O_GC} (Table S5). However, whether this finding was related to the potentially higher sensitivity of the QCL device or due to other variations in the sampling procedures was not resolved. Instead, we found that the disagreement between the GC and QCL method was likely related to ambient N_2O concentrations in the chamber headspace that remained

Deleted:
Deleted: , which
Deleted: general
Deleted: a chamber
Deleted: whereas
Deleted: At the annual scale
Moved down [1]: Jones et al., 2011;
Moved (insertion) [1]
Deleted: ;
Deleted: fluxes
Formatted: Subscript
Deleted: when using the static chamber method
Deleted: possible

between 300-400 ppb and showed a non-linear response with time, regardless of which analytic device was used. This might have resulted in the calculation of very small but apparent positive and negative F_{N2O}, when in fact the actual flux was zero (*Type I error* as defined by Parkin et al. (2012)). The integration of C_{N2O} with time to calculate F_{N2O}, therefore, likely included this error; rather than being caused by uncertainties associated with the measurement procedures or choice of analytic device (Kroon et al., 2008). The deviation between control site (AN_0) and treatment F_{N2O} (AN_{300}, AN_{600}, AN_{900}) has to be taken into account when evaluating the above results and mathematical principles (Sect. 3.2.2). Furthermore, since static chamber measurements often include near-ambient C_{N2O}, and likewise fluxes equal or near-zero, F_{N2O} from control plots were kept in the manuscript for completeness.

3.2.4 Cumulative N_2O emissions

Cumulative N_2O emissions across the seven-day campaign were quantified slightly greater for the GC (E_{N2O_GC}) than the QCL (E_{N2O_QCL}) method. The mean difference between E_{N2O_GC} and E_{N2O_QCL} for the control (AN_0) and each treatment, AN_{300}, AN_{600} and AN_{900}, was -0.011, +0.0023, +0.050 and +0.028 kg N ha^{-1}, respectively. This was a difference of less than 4 % in total N_2O emissions during deployment (Fig. 5).

[FIGURE 5 ABOUT HERE]

3.3 Measurement performance of QCL analysis

The measurement precision of QCL and, particularly, GC have been generally well-reviewed (de Klein et al., 2015; Lebegue et al., 2016; Rapson and Dacres, 2014). Gas chromatographs can be as precise as < 0.5 ppb (van der Laan et al., 2009; Rapson and Dacres, 2014) while the precision of a QCL is about 0.3 ppb for measurements made at 10 Hz, and 0.05 ppb for 1 Hz; but in some cases might be even higher (~1 ppt) (Curl et al., 2010; Rapson and Dacres, 2014; Savage et al., 2014). Zellweger et al. (2019), for instance, used laboratory QCL for the calibration of N_2O reference standards to inform the internationally accepted calibration scale of the Global Atmosphere Watch Programme of the World Meteorological Organisation. Similarly, Rosenstock et al. (2013) verified the accuracy and precision of different photoacoustic spectrometers based on laboratory QCL. However, the analytic precision can also depend on factors other than the technical performance of the analyser itself. Rannik et al. (2015) indicated that the performance (and thus the precision of F_{N2O}) of an analyser to measure gas samples from static chamber is likely more limited by the precision of the chamber system than by errors related to the analysis or post-processing of the data. Imprecisions might be caused by several factors, e.g. chamber type and dimension, experimental set-up, deployment time and preferred sampling method, all of which can affect the overall flux detection limit (Sect. 3.2.2). In contrast, the sources of uncertainty in our study were most likely related to 1) insufficient evacuation of Exetainers leading to the sporadic dilution of gas samples and N_2O standards; and 2) variation of 1 mL sample volumes when injected into the QCL. In practice, these might not have always been equal to 1 mL and, thus, could have resulted in slight variations of output peak area. In agreement with our observations, de Klein et al. (2015) found that half the uncertainty of static chamber measurements

Deleted: Hence
Deleted: , t
Deleted: of F_{N2O} determined at
Deleted: s
Deleted: from
Deleted: S
Deleted: F_{N2O}
Deleted: the purpose of
Deleted: ,
Deleted: ,
Deleted: The precision of common
Deleted: C analysers
Deleted: is
Deleted: Rapson and Dacres, 2014;
Deleted: was found to be
Deleted: preferred lab-based QCL to
Deleted: y
Deleted: However
Deleted: was also found to
Deleted:
Deleted: analytic device
Deleted: static chamber derived
Deleted: itself
Deleted: would lead to
Deleted: differences in
Deleted: :
Deleted: which
Deleted: in practice
Deleted: these
Deleted: measurement

could be explained by the variability of sample volume in the Exetainers. The inclusion of a fixed volume sample loop, e.g. when injecting gas samples into the QCL, might help to reduce this source of error in the future.

The QCL analysis of our study was conducted in a temperature- and pressure-controlled environment, where variations in these parameters were unlikely, and the variation in temperature expected to be less than 0.02 ppb $°C^{-1}$ (Lebegue et al., 2016). Nonetheless, we recommend a constant baseline flow of N_2 carrier gas at constant pressure (slightly higher than ambient) and temperature for manual injections made into the QCL device to avoid uncertainty affecting output peak areas. Depending on the QCL EC system, an initial lag time of 10 to 30 min before injections might be required to assemble the operational set-up (Section 2.2.3) and ensure sufficient stabilisation of pressure and temperature in the QCL sample cell. Given a flow rate of 1 L min^{-1}, rapid injections into the QCL should become possible shortly afterwards with a delay between single injections of 1 mL sample volumes of not more than 5 to 8 sec. Sample concentrations of the same volume but at N_2O concentrations > 20 ppm required a longer delay time between individual injections (> 20 sec) to ensure sufficient flushing of the QCL sample cell and avoid cross-contamination (Fig. S1). The identification of suitable delay times was straight forward in our case and could be easily accessed in real-time by visually examining the peak progression in TDLWintel. When observing the peak progression, for instance, it became noticeable that the injection of blanks (N_2 carrier gas) did not result in any changes in baseline flow. However, we did not determine the extent to which spontaneous but small variations in the flow rate of N_2 carrier gas would have affected our resulting output peak areas. Further uncertainties might have been associated with processing and curve-fitting procedures applied to the raw dataset in MATLAB, and likely resulted in small underestimations of true output peak areas.

3.4 QCL injections

3.4.1 The concept of bioequivalence

Using the Pearson correlation coefficient and the coefficient of determination for comparing two or more quantitative methods is a generally preferred approach in the field of N_2O research. Comparisons of different methods for N_2O analysis made in the literature most commonly used orthogonal (Jones et al., 2011) and linear regression (Cowan et al., 2014; Brümmer et al., 2017; Tallec et al., 2019), Students t-tests (Christiansen et al., 2015) or were based on raw data (Savage et al., 2014). However, correlation studies as such have limitations when assessing the comparability between two methods since a correlation analysis only identifies the relationship between two variables, not the difference (Giavarina, 2015). Bland Altman and bioequivalence statistics overcome this limitation by assessing the degree of agreement between methods.

An important aspect of statistical hypothesis testing is that the null hypothesis is never accepted. But failure to reject the null hypothesis is not the same as proving no difference. A bioequivalence analysis allows the statistical assessment of whether two methods (e.g. measurement devices, drug treatment) are effectively the same. Central to a bioequivalence analysis is the "equivalence range" that defines the size of the acceptable difference for which the values are similar enough to be considered equivalent. This becomes important when considering that even with the most precise analytical design and the most tightly

Deleted: gas
Deleted: sample
Deleted: As t
Deleted: he
Deleted: N_2O
Deleted: using QCL
Deleted: pressure
Deleted: . The temperature dependency of N_2O analysis by QCL was described as being linear by Lebegue et al. (2016) with variations
Deleted: To reduce the uncertainty of output peak area,
Deleted: w
Deleted: EC
Deleted: in order
Deleted:
Deleted: only
Deleted: at
Deleted: N_2O
Deleted: enable
Deleted: to
Deleted: easily
Deleted: of
Deleted: extend
Deleted: the
Deleted: of true output peak areas
Deleted: also
Deleted: curve
Deleted: that
Deleted: led
Deleted: to
Deleted: Brümmer et al., 2017;
Deleted: assessment

controlled experimental conditions, e.g. F_{N2O_GC} and F_{N2O_QCL} will never be exactly the same (Rani and Pargal, 2004). However, if the difference is sufficiently small for 'practical purposes', F_{N2O_GC} and F_{N2O_QCL} can be considered effectively the same. Here, accepted evidence of bioequivalence for F_{N2O_QCL} was that the 90 % confidence interval of the difference F_{N2O_QCL}-F_{N2O_GC} (corresponding to a test with size 0.05) was within a ± 5 % difference of F_{N2O_GC}. The equivalence range will vary depending on the objective of the research or guidelines provided by a regulatory authority, but commonly does not exceed ± 20 % (Westlake, 1988; Rani and Pargal, 2004; Ring et al., 2019). In our study, a small equivalence range of ± 5 % was preferred to test the difference between F_{N2O_QCL} and F_{N2O_GC} since such recommendations did not exist.

Overall, our results showed that F_{N2O_GC} and F_{N2O_QCL} from AN_{300}, AN_{600} and AN_{900} plots provided evidence of bioequivalence. The 90 % confidence intervals of the difference (F_{N2O_GC}-F_{N2O_QCL}) were quantified 0.127 (AN_{300}), 0.185 (AN_{600}) and -0.043 (AN_{900}) nmol N_2O m^{-2} s^{-1} and well within the pre-defined equivalence range of ± 5 % (Fig. 6e, Table S6). At control sites (AN_0), F_{N2O_GC} and F_{N2O_QCL} did not provide evidence for bioequivalence. However, the failure to establish equivalence for AN_0 sites was due to the overall limitation of the static chamber method to provide 'real' F_{N2O}, rather than based on a failure of the statistical principle (Sect. 3.2.3). On the contrary, when tested for C_{N2O} instead of F_{N2O}, equivalence was confirmed for t_0 and t_{15} but did not apply to t_{30} and t_{45} (Fig. 6a). Again, failure to establish equivalence was likely related to limitations of the static chamber method which, in this case, were indicated by the lower boundary of the 90 % CI remaining outside the predefined equivalence ranges. Another possible reason for not accepting equivalence for GC and QCL derived data at AN_0 sites could have been the maximum acceptable difference between the two methods itself. We defined (Sect. 2.5) that this difference had to be within ± 5 % of the mean difference of the standard method (i.e. GC). It has to be taken into consideration that the accepted evidence of bioequivalence would have led to different results if the percentage mean difference had been set to, for instance, ± 10 %. Accepting a greater mean difference between the two methods would have consequently resulted in evidencing bioequivalence for C_{N2O_GC} and C_{N2O_QCL} even at ambient concentrations. More generally, we found that positive values of the 90 % CI of the difference indicated that the difference between the two methods (GC-QCL) resulted in higher C_{N2O_GC} and F_{N2O_GC}. Negative values, instead, showed that the difference GC-QCL led C_{N2O_QCL} and F_{N2O_QCL} values to be greater than those from C_{N2O_GC} and F_{N2O_GC}, but in either case, the overall difference between the two methods did not exceed ± 0.1 ppm for C_{N2O} and ± 0.38 nmol N_2O m^{-2} s^{-1} for F_{N2O} (Fig. 6e).

[FIGURE 6 ABOUT HERE]

To the best of our knowledge, bioequivalence has not broadly been applied in the greenhouse gas literature to identify and to discuss the range at which a difference in F_{N2O_GC} and F_{N2O_QCL} could be considered relevant when using different analytical methods. However, defining the magnitude of F_{N2O} (e.g. in nmol N_2O m^{-2} s^{-1}) at which a unit difference would become relevant is important when using different methods to quantify, compare and, ultimately, upscale N_2O emissions. We, thus, recommend bioequivalence or other statistical approaches (e.g. Bland Altman) for more formally assessing the agreement between two methods in the future.

Deleted: an

Deleted: ¶

Deleted: ; Westlake, 1988

Deleted:

Deleted: ;

Deleted: for

Deleted: that

Deleted: was

Deleted: However

Deleted: , i

Deleted: Consequently, a

Deleted: determining

Deleted: higher

Deleted: .

Deleted: The

Deleted: Defining

Deleted: actually

Deleted: , however,

Deleted: therefore

3.4.2 Strengths and weaknesses

The employment of a QCL analyser proposes an alternative approach for the injection of N_2O samples taken from static chambers, particularly as F_{N2O_QCL} were generally equivalent to F_{N2O_GC}. Using a QCL for manual injections can be conducted without much disruption to other measurements (e.g. EC or automated chambers) and, therefore, helps justify the initially higher capital and general running costs involved with operating a QCL device. Additional labour effort and time associated with sample storage and transport necessary for laboratory GC do not necessarily apply for field-based injections into a QCL. Once established, a QCL system has relatively low maintenance and offers a straightforward application for manual injections in addition to EC or other measurement tasks. In our study, the assembly of the injection set-up required little equipment and was installed within 30 min. This allowed for a rapid analysis after chamber sampling without greatly interfering with other measurements, i.e. EC, that were offline during the time of injection into the QCL. To collectively inject a great number of samples turned out to be highly beneficial to minimise the downtime of the EC measurements, in our case, and also helped to reduce other interferences made to the QCL. For instance, we were able to inject a total of around 700, 1 mL samples (432 samples, 268 standards) within four hours (Table 1). Prior to QCL analysis, these samples had been kept in septum-sealed Exetainers that can store gas samples for up to 28 days at any temperature between -10 and 25°C (Faust and Liebig, 2018). We acknowledge that a sporadic dilution of our samples might still have occurred due to storage in and potentially insufficient evacuation of Exetainers which, in turn, could have affected subsequent GC and QCL analyses (de Klein et al., 2015). Despite this potential source of uncertainty, storing N_2O samples in Exetainers enabled repeated injections and allowed to postpone the analysis if EC measurements were of higher importance or if the weather conditions (e.g. precipitation) were unsuitable. Similar to GC, QCL injections required consumables (N_2 carrier gas, N_2O standards) but, in contrast, time and costs associated with laboratory work were substantially less (Table 1).

[TABLE 1 ABOUT HERE]

4 Conclusion

Previously, QCL had been used either in conjunction with EC or coupled to automated chambers. Here, we showed that one QCL device could be used as a practical tool for the analysis of static chamber derived N_2O samples without major disruption to these other measurement tasks. We found treatment N_2O concentrations (C_{N2O_QCL}) and fluxes (F_{N2O_QCL}) from QCL agreed with results based on laboratory GC (C_{N2O_GC}, F_{N2O_GC}). The percentage difference between treatment F_{N2O_GC} and F_{N2O_QCL} was not smaller than -11.2 % and not greater than +9.2 % with a mean difference between the two of only 0.1 nmol N_2O m^{-2} s^{-1}. A deviation between the GC and QCL methods was determined only for close to zero F_{N2O} at control plots where F_{N2O_GC} and F_{N2O_QCL} values were found outside the predefined equivalence range. However, this was likely due to the calculation of very small but apparent positive and negative F_{N2O} (when in fact the actual flux was zero), rather than due to uncertainties caused by a weakness of the GC or QCL analysis. Equivalence was evidenced for all other F_{N2O_GC} and F_{N2O_QCL} and confirmed that GC and QCL data were for practical purposes the same. We found that using Bland Altman and bioequivalence statistics

Deleted: offers
Deleted: the purpose of
Deleted: s
Deleted:
Deleted: such as
Deleted: manual
Deleted: Nonetheless, we recommend to c
Deleted: N_2O
Deleted: in order
Deleted: to
Deleted: into the QCL
Deleted: N_2O
Deleted: for both
Deleted: due to sample storage in and insufficient evacuation of sample Exetainers
Deleted: also
Deleted: from the same sample for multiple times
Deleted: sample injections at suitable times, i.e.
Deleted: postponing
Deleted: did not support
Deleted: manual injections into the QCL
Deleted: D
Deleted: ;
Deleted: being caused by
Deleted: related
Deleted: to
Deleted: itself
Deleted: , i.e. it was

in addition to regression analysis served the comparison of GC and QCL particularly well. Yet, these two statistical approaches have not broadly been used in the field of greenhouse gas research to compare different analytical methods or to discuss the magnitude at which a difference in F_{N2O} would become relevant. Since correlation studies identify the relationship between two methods but not the difference, we recommend that bioequivalence or other suitable statistical approaches are used for more formally assessing the agreement between two methods. Finally, QCL offers great potential to interlink different methods of gas measurements across different temporal and spatial scales. In the future, this capability might not only be important for rapid field analysis of N_2O samples but equally also applies to the measurement of other gas species (e.g. CO_2, CH_4) and gas isotopomers of interest.

Deleted: , or other greenhouse gas fluxes,

Deleted: a

Data availability

Data were deposited at the University of Waikato Research Commons, see (Wecking et al., 2020b) https://researchcommons.waikato.ac.nz/handle/10289/13539

Supplements to this manuscript exist.

Author contributions

ARW, VC, JL and LS designed the experiment. ARW performed the fieldwork. ARW conducted the post-processing of GC and QCL data using MATLAB scripts, which based on the work from AW and DC. ARW performed the statistical analysis with inputs and contributions from VC. VC and LS commented on the results of the initial data analysis. ARW wrote and revised the manuscript with contributions from VC, AW, LL, JL, DC and LS.

Deleted:

Deleted: provided by

Competing interests

The authors declare that they have no conflict of interest.

Acknowledgements

This research was supported by the New Zealand Agricultural Greenhouse Gas Research Centre (NZAGRC), AgResearch Ruakura, DairyNZ and the University of Waikato. The authors would like to recognise the farm owners, Sarah and Ben Troughton, for their cooperation. Chris Morcom is thanked for his help in the fields and Emily Huang from NZ-NCNM for her all-embracing support regarding gas chromatography. Training notes on the concept of bioequivalence were gratefully received from Neil Cox. We would like to further acknowledge the continuous support from Aerodyne Research Ltd. in

maintaining and advancing our QCL EC systems. Finally, Cecile A. M. de Klein, Tom P. Moore and two anonymous reviewers are thanked for thoroughly revising the manuscript of this work.

Deleted: based

References

Baldocchi, D.: Measuring fluxes of trace gases and energy between ecosystems and the atmosphere – the state and future of the eddy covariance method, Global Change Biol., 20, 3600-3609, 10.1111/gcb.12649, 2014.

Bland, M. J., and Altman, D. G.: Statistical method for assessing agreement between two methods of clinical measurement, The Lancet, 327, 307-310, https://doi.org/10.1016/S0140-6736(86)90837-8, 1986.

Bouwman, A. F., Boumans, L. J. M., and Batjes, N. H.: Emissions of N2O and NO from fertilized fields: Summary of available measurement data, Global Biogeochem. Cycles, 16, 6-1, 2002.

Brümmer, C., Lyshede, B., Lempio, D., Delorme, J.-P., Rüffer, J. J., Fuß, R., Moffat, A. M., Hurkuck, M., Ibrom, A., Ambus, P., Flessa, H., and Kutsch, W. L.: Gas chromatography vs. quantum cascade laser-based N2O flux measurements using a novel chamber design, Biogeosciences, 14, 1365-1381, 10.5194/bg-14-1365-2017, 2017.

Butterbach-Bahl, K., Baggs, E. M., Dannenmann, M., Kiese, R., and Zechmeister-Boltenstern, S.: Nitrous oxide emissions from soils: how well do we understand the processes and their controls?, Philosophical transactions of the Royal Society of London. Series B, Biological sciences, 368, 20130122, 10.1098/rstb.2013.0122, 2013.

Cardenas, L. M., Bhogal, A., Chadwick, D. R., McGeough, K., Misselbrook, T., Rees, R. M., Thorman, R. E., Watson, C. J., Williams, J. R., Smith, K. A., and Calvet, S.: Nitrogen use efficiency and nitrous oxide emissions from five UK fertilised grasslands, Sci. Total Environ., 10.1016/j.scitotenv.2019.01.082, 2019.

Chadwick, D. R., Cardenas, L., Misselbrook, T. H., Smith, K. A., Rees, R. M., Watson, C. J., McGeough, K. L., Williams, J. R., Cloy, J. M., Thorman, R. E., and Dhanoa, M. S.: Optimizing chamber methods for measuring nitrous oxide emissions from plot-based agricultural experiments, Eur. J. Soil Sci., 65, 295-307, 10.1111/ejss.12117, 2014.

Christiansen, J. R., Korhonen, J. F. J., Juszczak, R., Giebels, M., and Pihlatie, M.: Assessing the effects of chamber placement, manual sampling and headspace mixing on CH4 fluxes in a laboratory experiment, Plant and Soil, 343, 171-185, 10.1007/s11104-010-0701-y, 2011.

Christiansen, J. R., Outhwaite, J., and Smukler, S. M.: Comparison of CO2, CH4 and N2O soil-atmosphere exchange measured in static chambers with cavity ring-down spectroscopy and gas chromatography, Agric. For. Meteorol., 211-212, 48-57, https://doi.org/10.1016/j.agrformet.2015.06.004, 2015.

Cowan, N., Levy, P., Maire, J., Coyle, M., Leeson, S. R., Famulari, D., Carozzi, M., Nemitz, E., and Skiba, U.: An evaluation of four years of nitrous oxide fluxes after application of ammonium nitrate and urea fertilisers measured using the eddy covariance method, Agric. For. Meteorol., 280, 107812, https://doi.org/10.1016/j.agrformet.2019.107812, 2020.

Cowan, N. J., Famulari, D., Levy, P. E., Anderson, M., Bell, M. J., Rees, R. M., Reay, D. S., and Skiba, U. M.: An improved method for measuring soil N2O fluxes using a quantum cascade laser with a dynamic chamber, Eur. J. Soil Sci., 65, 643-652, 10.1111/ejss.12168, 2014.

Curl, R. F., Capasso, F., Gmachl, C., Kosterev, A. A., McManus, B., Lewicki, R., Pusharsky, M., Wysocki, G., and Tittel, F. K.: Quantum cascade lasers in chemical physics, Chem. Phys. Lett., 487, 1-18, https://doi.org/10.1016/j.cplett.2009.12.073, 2010.

de Klein, C. A. M., Barton, L., Sherlock, R. R., Li, Z., and Littlejohn, R. P.: Estimating a nitrous oxide emission factor for animal urine from some New Zealand pastoral soils, Aust. J. Soil Res., 41, 381-399, 10.1071/SR02128, 2003.

de Klein, C. A. M., Harvey, M. J., Clough, T., Rochette, P., Kelliher, F., Venetera, R., Alfaro, M., and Chadwick, D.: Nitrous Oxide Chamber Methodology Guidelines. Version 1.1, Ministry of Primary Industries,, Wellington, 146, 2015.

Denmead, O.: Approaches to measuring fluxes of methane and nitrous oxide between landscapes and the atmosphere, Plant and Soil, 309, 5-24, 10.1007/s11104-008-9599-z, 2008.

Erisman, J. W., Galloway, J. N., Seitzinger, S., Bleeker, A., Dise, N. B., Petrescu, A. M. R., Leach, A. M., and de Vries, W.: Consequences of human modification of the global nitrogen cycle, Philosophical Transactions of the Royal Society B: Biological Sciences, 368, 10.1098/rstb.2013.0116, 2013.

Faust, D. R., and Liebig, M. A.: Effects of storage time and temperature on greenhouse gas samples in Exetainer vials with chlorobutyl septa caps, MethodsX, 5, 857-864, https://doi.org/10.1016/j.mex.2018.06.016, 2018.

Firestone, M. K., and Davidson, E. A.: Microbiological Basis of NO and N2O Production and Consumption in Soil, in: Exchange of Trace Gases between Terrestrial Ecosystems and the Atmosphere, edited by: Andreae, M. O., and Schmimmel, D. S., John Wiley & Sons Ltd, 7-21, 1989.

Flechard, C. R., Ambus, P., Skiba, U., Rees, R. M., Hensen, A., van Amstel, A., van Den Pol-van Dasselaar, A., Soussana, J. F., Jones, M., Clifton-Brown, J., Raschi, A., Horvath, L., Neftel, A., Jocher, M., Ammann, C., Leifeld, J., Fuhrer, J., Calanca, P., Thalman, E., Pilegaard, K., Di Marco, C., Campbell, C., Nemitz, E., Hargreaves, K. J., Levy, P. E., Ball, B. C., Jones, S. K., van de Bulk, W. C. M., Groot, T., Blom, M., Domingues, R., Kasper, G., Allard, V., Ceschia, E., Cellier, P., Laville, P., Henault, C., Bizouard, F., Abdalla, M., Williams, M., Baronti, S., Berretti, F., and Grosz, B.: Effects of climate and management intensity on nitrous oxide emissions in grassland systems across Europe, Agriculture, Ecosystems and Environment, 121, 135-152, 10.1016/j.agee.2006.12.024, 2007.

Giavarina, D.: Understanding Bland Altman analysis, Biochemia medica, 25, 141-151, 10.11613/BM.2015.015, 2015.

Hutchinson, G. L., and Mosier, A. R.: Improved Soil Cover Method for Field Measurement of Nitrous Oxide Fluxes1, Soil Sci. Soc. Am. J., 45, 311-316, 10.2136/sssaj1981.03615995004500020017x, 1981.

IPCC: Anthropogenic and Natural Radiative Forcing, in: Climate Change 2013: The Physical Science Basis. Contribution of Working Group I to the Fifth Assessment Report of the Intergovenmental Panel on Climate Change., edited by: Myhre, G., Shindell, D., Breon, F.-M., Collins, W., Fuglestvedt, J., Huang, J., Koch, D., Lamarque, J.-F., Lee, D., Mendoza, B., Nakajima, T., Robock, A., Stephens, G., Takemura, T., Zhang, H., Jacob, D., Ravishankara, A. R., and Shine, K. P., Cambidge UK and New York, NY, USA, 659-740, 2013.

Jones, S., Famulari, D., Marco, C., Nemitz, E., Skiba, U., Rees, R., and Sutton, M.: Nitrous oxide emissions from managed grassland: a comparison of eddy covariance and static chamber measurements, Atmos. Meas. Tech., 4, 2179–2194, 10.5194/amt-4-2179-2011, 2011.

Jones, S. K., Rees, R. M., Skiba, U. M., and Ball, B. C.: Influence of organic and mineral N fertiliser on N2O fluxes from a temperate grassland, Agriculture, Ecosystems and Environment, 121, 74-83, 10.1016/j.agee.2006.12.006, 2007.

Kroon, P., Hensen, A., Bulk, W., Jongejan, P., and Vermeulen, A.: The importance of reducing the systematic error due to non-linearity in N2O flux measurements by static chambers, Nutr. Cycling Agroecosyst., 82, 175-186, 10.1007/s10705-008-9179-x, 2008.

Lammirato, C., Lebender, U., Tierling, J., and Lammel, J.: Analysis of uncertainty for N2O fluxes measured with the closed-chamber method under field conditions: Calculation method, detection limit, and spatial variability, J. Plant Nutr. Soil Sci., 181, 78-89, 10.1002/jpln.201600499, 2018.

Lebegue, B., Schmidt, M., Ramonet, M., Wastine, B., Yver Kwok, C., Laurent, O., Belviso, S., Guemri, A., Philippon, C., Smith, J., and Conil, S.: Comparison of N2O analyzers for high-precision measurements of atmospheric mole fractions, Atmos. Meas. Tech., 9, 1221-1238, 10.5194/amt-9-1221-2016, 2016.

Liáng, L. L., Campbell, D. I., Wall, A. M., and Schipper, L. A.: Nitrous oxide fluxes determined by continuous eddy covariance measurements from intensively grazed pastures: Temporal patterns and environmental controls, Agriculture, Ecosystems & Environment, 268, 171-180, https://doi.org/10.1016/j.agee.2018.09.010, 2018.

Lundegard, H.: Carbon dioxide evolution of soil and crop growth, Soil Science, 23, 417-453, 1927.

Luo, J., Ledgard, S. F., and Lindsey, S. B.: Nitrous oxide emissions from application of urea on New Zealand pasture, N.Z. J. Agric. Res., 50, 1-11, 10.1080/00288230709510277, 2007.

Luo, J., Ledgard, S., Klein, C., Lindsey, S., and Kear, M.: Effects of dairy farming intensification on nitrous oxide emissions, Plant Soil, 309, 227-237, 10.1007/s11104-007-9444-9, 2008a.

Luo, J., Lindsey, S., and Ledgard, S.: Nitrous oxide emissions from animal urine application on a New Zealand pasture, Biol. Fertil. Soils, 44, 463-470, 10.1007/s00374-007-0228-4, 2008b.

Luo, J., Wyatt, J., van der Weerden, T. J., Thomas, S. M., de Klein, C. A. M., Li, Y., Rollo, M., Lindsey, S., Ledgard, S. F., Li, J., Ding, W., Qin, S., Zhang, N., Bolan, N. S., Kirkham, M. B., Bai, Z., Ma, L., Zhang, X., Wang, H., Liu, H., and Rys, G.: Potential Hotspot Areas of Nitrous Oxide Emissions From Grazed Pastoral Dairy Farm Systems, Advances in Agronomy, 145, 205-268, 10.1016/bs.agron.2017.05.006, 2017.

Mulvaney, R. L.: Extraction of exchangeable ammonium, nitrate and nitrite, in: Methods of soil analysis Part 3: chemical methods, edited by: Sparks, D. L., Page, A. L., Helmke, P. A., and Loeppert, R. H., 5.3, Soil Science Society of America, American Society of Agronomy, Madison, WI, 1129-1131, 1996.

Neftel, A., Flechard, C., Ammann, C., Conen, F., Emmenegger, L., and Zeyer, K.: Experimental assessment of N2O background fluxes in grassland systems, Tellus B Chem Phys Meteorol, 59, 470-482, 10.1111/j.1600-0889.2007.00273.x, 2007.

Nelson, D. D., McManus, B., Urbanski, S., Herndon, S., and Zahniser, M. S.: High precision measurements of atmospheric nitrous oxide and methane using thermoelectrically cooled mid-infrared quantum cascade lasers and detectors, Spectrochim. Acta, Part A, 60, 3325-3335, https://doi.org/10.1016/j.saa.2004.01.033, 2004.

Nemitz, E., Mammarella, I., Ibrom, A., Aurela, M., Burba, G., Dengel, S., Gielen, B., Grelle, A., Heinesch, B., Herbst, M., Hörtnagl, L., Klemedtsson, L., Lindroth, A., Lohila, A., McDermitt, K. D., Meier, P., Merbold, L., Nelson, D., Nicolini, G., and Zahniser, M.: Standardisation of eddy-covariance flux measurements of methane and nitrous oxide, 32, 517-549, 10.1515/intag-2017-0042, 2018.

Nicolini, G., Castaldi, S., Fratini, G., and Valentini, R.: A literature overview of micrometeorological CH4 and N2O flux measurements in terrestrial ecosystems, Atmos. Environ., 81, 311-319, https://doi.org/10.1016/j.atmosenv.2013.09.030, 2013.

National Climate Database. National Institute of Water and Atmospheric Research: http://cliflo.niwa.co.nz/, 2018.

Parkin, T. B., and Venterea, R. T.: Chamber-based trace gas flux measurements, USDA-ARS GRACEnet Project Protocols, Chapter 3, 2010.

Parkin, T. B., Venterea, R. T., and Hargreaves, S. K.: Calculating the Detection Limits of Chamber-based Soil Greenhouse Gas Flux Measurements, J. Environ. Qual., 41, 705-715, 10.2134/jeq2011.0394, 2012.

Patterson, S., and Jones, B.: Interdisciplinary statistics. Bioequivalence and statistics in clinical pharmacology, Taylor & Francis Group, Boca Raton, FL, 2006.

Pavelka, M., Acosta, M., Kiese, R., Altimir, N., Bruemmer, C., Crill, P., Darenova, E., Fuß, R., Gielen, B., Graf, A., Klemedtsson, L., Lohila, A., Longdoz, B., Lindroth, A., Nilsson, M., Marañón-Jiménez, S., Merbold, L., Montagnani, L., Peichl, M., and Kutsch, W. L.: Standardisation of chamber technique for CO2, N2O and CH4 fluxes measurements from terrestrial ecosystems, Int. Agrophys., 32, 569-587, 10.1515/intag-2017-0045, 2018.

Rani, S., and Pargal, A.: Bioequivalence: An overview of statistical concepts, Indian Journal of Pharmacology, 36, 209-216, 2004.

Rannik, Ü., Haapanala, S., Shurpali, N. J., Mammarella, I., Lind, S., Hyvönen, N., Peltola, O., Zahniser, M., Martikainen, P. J., and Vesala, T.: Intercomparison of fast response commercial gas analysers for nitrous oxide flux measurements under field conditions, Biogeosciences, 12, 415-432, 10.5194/bg-12-415-2015, 2015.

Rapson, T. D., and Dacres, H.: Analytical techniques for measuring nitrous oxide, "TrAC, Trends Anal. Chem. ", 54, 65-74, http://dx.doi.org/10.1016/j.trac.2013.11.004, 2014.

Ravishankara, J. S., Daniel, R. W., and Portmann, R. W.: Nitrous oxide (N2O): The dominant ozone-depleting substance emitted in the 21st century, Science, 326, 123-125, 10.1126/science.1176985, 2009.

Reay, D. S., Davidson, E. A., Smith, K. A., Smith, P., Melillo, J. M., Dentener, F., and Crutzen, P. J.: Global agriculture and nitrous oxide emissions, Nature Climate Change, 2, 410, 10.1038/nclimate1458
https://www.nature.com/articles/nclimate1458#supplementary-information, 2012.

Rees, R., Augustin, J., Alberti, G., Ball, B., Boeckx, P., Cantarel, A., Castaldi, S., Chirinda, N., Chojnicki, B., Giebels, M., Gordon, H., Grosz, B., Horvath, L., Juszczak, R., Klemedtsson, Å., Klemedtsson, L., Medinets, S., Machon, A., Mapanda, F., Nyamangara, J., Olesen, J., Reay, D., Sanchez, L., Cobena, A., Smith, K., Sowerby, A., Sommer, M., Soussana, J., Stenberg, M., Topp, C., van Cleemput, O., Vallejo, A., Watson, C., and Wuta, M.: Nitrous oxide emissions from European agriculture - an analysis of variability and drivers of emissions from field experiments, Biogeosciences, 10, 2671, 10.5194/bg-10-2671-2013, 2013.

Ring, A., Lang, B., Kazaroho, C., Labes, D., Schall, R., and Schütz, H.: Sample size determination in bioequivalence studies using statistical assurance, British Journal of Clinical Pharmacology, 85, 2369-2377, 10.1111/bcp.14055, 2019.

Rochette, P., and Bertrand, N.: Soil air sample storage and handling using polypropylene syringes and glass vials, Can. J. Soil Sci., 83, 631-637, 10.4141/S03-015, 2003.

Rochette, P., and Eriksen-Hamel, N.: Chamber Measurements of Soil Nitrous Oxide Flux: Are Absolute Values Reliable?, Soil Sci. Soc. Am. J., 72, 331-342, 10.2136/sssaj2007.0215, 2008.

Rochette, P.: Towards a standard non-steady-state chamber methodology for measuring soil N2O emissions, Anim. Feed Sci. Technol., 166, 141-146, http://dx.doi.org/10.1016/j.anifeedsci.2011.04.063, 2011.

Rosenstock, T. S., Diaz-Pines, E., Zuazo, P., Jordan, G., Predotova, M., Mutuo, P., Abwanda, S., Thiong'o, M., Buerkert, A., Rufino, M. C., Kiese, R., Neufeldt, H., and Butterbach-Bahl, K.: Accuracy and precision of photoacoustic spectroscopy not guaranteed, Global Change Biol., 19, 3565-3567, 10.1111/gcb.12332, 2013.

Savage, K., Phillips, R., and Davidson, E.: High temporal frequency measurements of greenhouse gas emissions from soils, Biogeosciences, 11, 2709-2720, 10.5194/bg-11-2709-2014, 2014.

Selbie, D. R., Buckthought, L. E., and Shepherd, M. A.: Chapter Four - The Challenge of the Urine Patch for Managing Nitrogen in Grazed Pasture Systems, Adv. Agron., 129, 229-292, https://doi.org/10.1016/bs.agron.2014.09.004, 2015.

Tallec, T., Brut, A., Joly, L., Dumelié, N., Serça, D., Mordelet, P., Claverie, N., Legain, D., Barrié, J., Decarpenterie, T., Cousin, J., Zawilski, B., Ceschia, E., Guérin, F., and Le Dantec, V.: N2O flux measurements over an irrigated maize crop: A comparison of three methods, Agric. For. Meteorol., 264, 56-72, https://doi.org/10.1016/j.agrformet.2018.09.017, 2019.

Thompson, R. L., Lassaletta, L., Patra, P. K., Wilson, C., Wells, K. C., Gressent, A., Koffi, E. N., Chipperfield, M. P., Winiwarter, W., Davidson, E. A., Tian, H., and Canadell, J. G.: Acceleration of global N2O emissions seen from two decades of atmospheric inversion, Nature Climate Change, 10.1038/s41558-019-0613-7, 2019.

van der Laan, S., Neubert, R. E. M., and Meijer, H. A. J.: A single gas chromatograph for accurate atmospheric mixing ratio measurements of CO2, CH4, N2O, SF6 and CO, Atmos. Meas. Tech., 2, 549-559, 2009.

van der Weerden, T. J., Luo, J., de Klein, C. A. M., Hoogendoorn, C. J., Littlejohn, R. P., and Rys, G. J.: Disaggregating nitrous oxide emission factors for ruminant urine and dung deposited onto pastoral soils, Agriculture, Ecosystems and Environment, 141, 426-436, 10.1016/j.agee.2011.04.007, 2011.

van der Weerden, T. J., Clough, T. J., and Styles, T. M.: Using near-continuous measurements of N2O emission from urine-affected soil to guide manual gas sampling regimes, N.Z. J. Agric. Res., 56, 60-76, 10.1080/00288233.2012.747548, 2013.

Velthof, G. L., Jarvis, S. C., Stein, A., Allen, A. G., and Oenema, O.: Spatial variability of nitrous oxide fluxes in mown and grazed grasslands on a poorly drained clay soil, Soil Biol. Biochem., 28, 1215-1225, https://doi.org/10.1016/0038-0717(96)00129-0, 1996.

Wecking, A. R., Wall, A. M., Liáng, L. L., Lindsey, S. B., Luo, J., Campbell, D. I., and Schipper, L. A.: Reconciling annual nitrous oxide emissions of an intensively grazed dairy pasture determined by eddy covariance and emission factors, Agriculture, Ecosystems & Environment, 287, 106646, https://doi.org/10.1016/j.agee.2019.106646, 2020a.

Wecking, A. R., Wall, A. M., Liáng, L. L., Lindsey, S. B., Luo, J., Campbell, D. I., and Schipper, L. A.: Dataset for "A novel injection technique: using a field-based quantum cascade laser for the analysis of gas samples derived from static chamber". https://researchcommons.waikato.ac.nz/handle/10289/13539, 2020b.

Westlake, W. J.: Bioavailability and bioequivalence of pharmaceutical formulations, in: Biopharmaceutical Statistics for Drug Development, edited by: Peace, K. E., Marcel Dekker, New York, 329-352, 1988.

Zellweger, C., Steinbrecher, R., Laurent, O., Lee, H., Kim, S., Emmenegger, L., Steinbacher, M., and Buchmann, B.: Recent advances in measurement techniques for atmospheric carbon monoxide and nitrous oxide observations, Atmos. Meas. Tech., 12, 5863-5878, 10.5194/amt-12-5863-2019, 2019.

List of figures

Figure 1: Schematic illustration of how to use a field-based QCL for EC measurements and manual injections. (1) shows the main components of the QCL EC system; (2) provides an example of a static chamber from which N_2O samples were taken and stored in (3) pre-evacuated glass vials. Once the set-up for manual injections (4) was assembled and the QCL air-inlet (5) adjusted from drawing ambient air through the EC sample line (inlet 1) to drawing air via the injection tube (inlet 2), the QCL was readily set-up for receiving injections of N_2O samples and associated standards through the injection port. The data output (6) was immediate allowing processing and data evaluation on the day of chamber sampling.

Figure 2: Fluxes of nitrous oxide (F_{N2O}) determined from (a) gas chromatography (F_{N2O_GC}) and (b) quantum cascade laser absorption spectrometry (F_{N2O_QCL}). Symbols depict mean F_{N2O} and marker shading displays the rate of ammonium nitrate (AN) applied: AN_0 (black squares), AN_{300} (dark grey diamonds), AN_{600} (light grey upside-down triangles) and AN_{900} (white triangles). Error bars illustrate the standard error of the mean (SEM) across the three replicates of the same treatment. Note that flux measurements on 12 and 15 September were conducted twice daily (10 AM and 12 PM) and that the time scale on the x-axis, therefore, is discrete. Soil water-filled pore space (WFPS) and mineral nitrogen (N_{min}) contents associated with flux measurements are provided in the supplementary material, Table S3.

Figure 3: Orthogonal regression analysis of standardised N_2O concentrations (C_{N2O}) and fluxes (F_{N2O}). Data were distinguished by their analytic source of origin, i.e. GC (C_{N2O_GC}, F_{N2O_GC}) and QCL (C_{N2O_QCL}, F_{N2O_QCL}). The regression analysis included all C_{N2O} in (a) but only those C_{N2O} measured at control sites (AN_0) in panel (c). The orthogonal regression analysis was repeated for standardised F_{N2O} with (b) showing all F_{N2O_GC} and F_{N2O_QCL}, and (d) depicting the orthogonal regression for AN_0 fluxes only. Ordinary least squares (dotted light grey line) resulted from the regression of Y on X; inverse least squares from the regression of X on Y (long dotted dark grey line). The major axis (black line) based on orthogonal regression of Y and X using a principal component analysis. Here, the squared residuals perpendicular to the line are minimised. Note, for the purpose of illustration axes in panel (c) and (d) have different scales. Table S4 in the supplements provides further results.

Figure 4: Bland Altman plots showing the difference between the GC and QCL method expressed as the percentage difference of the standard method A (F_{N2O_GC}) and the new method B (F_{N2O_QCL}) on the y-axis [((A-B)/mean)× 100] versus the mean of A and B on the x-axis. The limits of agreement are represented by continuous lines at ±1.96 standard deviation (SD) of the percentage difference. The inset (panel b) illustrates the same data but excludes F_{N2O_GC} and F_{N2O_QCL} from control (AN_0) sites. The percentage mean difference (bias) between F_{N2O_GC} and F_{N2O_QCL}, i.e. method A and B, is indicated by the gap between the dashed line (line of equality, which is not at zero) and an imaginary line parallel to the dashed line at y = 0. This figure is

Deleted: through

Formatted: Subscript

Deleted: of

Deleted: s

based on individual F_{N2O} (all treatment replicates). Results for mean F_{N2O} across replicates of the same treatment are provided in the supplements, see Table S5.

Figure 5: Cumulative N_2O emissions from each treatment (AN_{300}, AN_{600}, AN_{900}) and the control (AN_0) in kg N_2O-N ha^{-1} at the end of the campaign. Data are distinguished into GC (black bars) and QCL (grey bars) budgets. Error bars quantify the standard error of the mean (SEM). The absolute difference in kg N_2O-N ha^{-1} between the two budgets (GC-QCL) is highlighted by the number on the top of each bar-couple.

Figure 6: Bioequivalence analysis for N_2O concentrations (C_{N2O}) in (a-d) and N_2O fluxes (F_{N2O}) in (e) with GC defined as the standard method. C_{N2O} and F_{N2O} based on QCL analysis were considered bioequivalent when the 90 % confidence interval (CI) of the difference between QCL and GC (x-axis) was completely within the predefined ± 5 % bioequivalence range of the difference of the standard method. The bioequivalence analysis was distinguished for C_{N2O} by sampling interval (t_0 ,t_{15} ,t_{30} , t_{45}) and treatment with panel (a) showing results for control sites (AN_0) and panels (b), (c) and (d) for AN_{300}, AN_{600} and AN_{900} treatment sites. Similarly, a bioequivalence analysis was conducted for F_{N2O} in panel (e) and distinguished by AN application rate on the y-axis.

List of tables

Table 1: The GC and QCL methods in comparison. Details provided in the table relate to in this study and information provided were not generalised. NZD = New Zealand dollars.

Deleted: of
Deleted: N_2O
Deleted: at
Deleted: determined
Deleted: , here
Deleted: Comparison of the
Deleted: injection
Deleted: .
Deleted: below
Deleted: specifically
Deleted: the application of the two techniques
Deleted: (i.e. have not been
Deleted:)

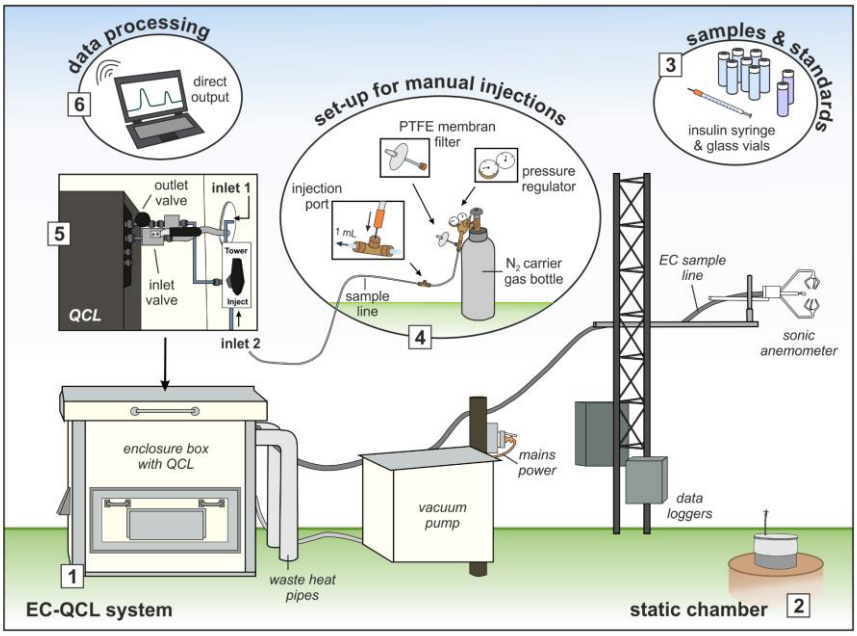

Figure 1: Schematic illustration of how to use a field-based QCL for EC measurements and manual injections. (1) shows the main components of the QCL EC system; (2) provides an example of a static chamber from which N_2O samples were taken and stored in (3) pre-evacuated glass vials. Once the set-up for manual injections (4) was assembled and the QCL air-inlet (5) adjusted from drawing ambient air through the EC sample line (inlet 1) to drawing air via the injection tube (inlet 2), the QCL was readily set-up for receiving injections of N_2O samples and associated standards through the injection port. The data output (6) was immediate allowing processing and data evaluation on the day of chamber sampling.

Deleted: through

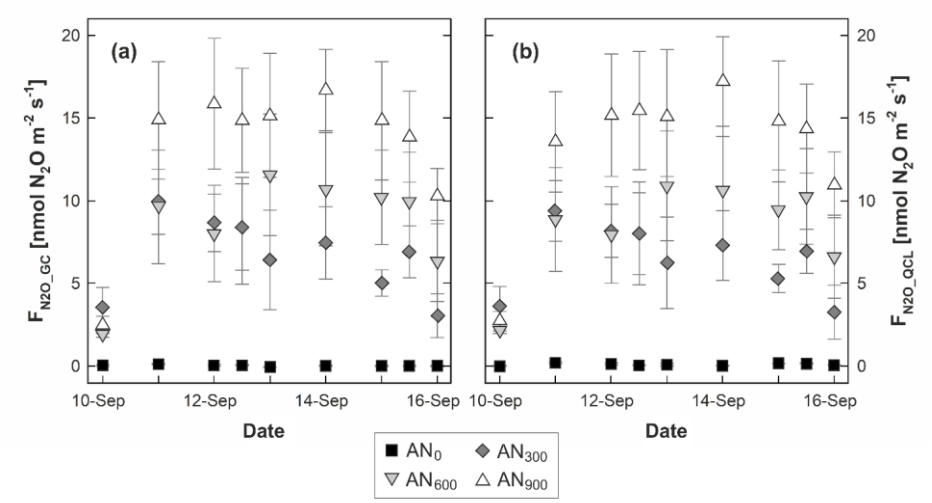

Figure 2: Fluxes of nitrous oxide (F_{N2O}) determined from (a) gas chromatography (F_{N2O_GC}) and (b) quantum cascade laser absorption spectrometry (F_{N2O_QCL}). Symbols depict mean F_{N2O} and marker shading displays the rate of ammonium nitrate (AN) applied: AN_0 (black squares), AN_{300} (dark grey diamonds), AN_{600} (light grey upside-down triangles) and AN_{900} (white triangles). Error bars illustrate the standard error of the mean (SEM) across the three replicates of the same treatment. Note that flux measurements on 12 and 15 September were conducted twice daily (10 AM and 12 PM) and that the time scale on the x-axis, therefore, is discrete. Soil water-filled pore space (WFPS) and mineral nitrogen (N_{min}) contents associated with flux measurements are provided in the supplementary material, Table S3.

Formatted: Subscript

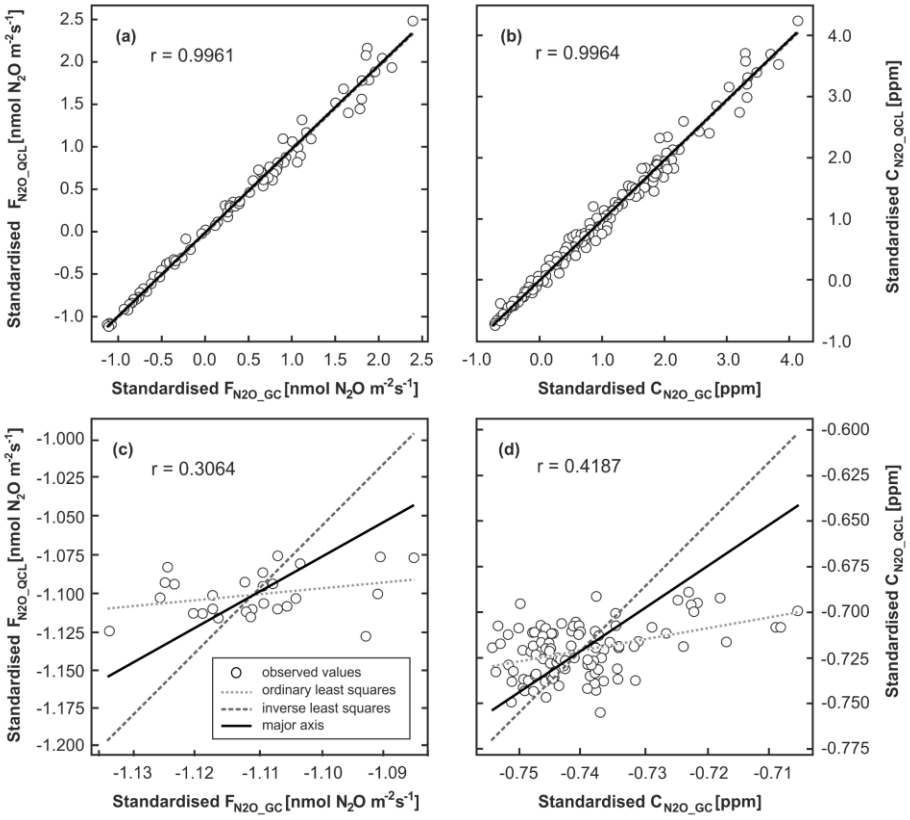

Figure 3: Orthogonal regression analysis of standardised N_2O concentrations (C_{N2O}) and fluxes (F_{N2O}). Data were distinguished by their analytic source of origin, i.e. GC (C_{N2O_GC}, F_{N2O_GC}) and QCL (C_{N2O_QCL}, F_{N2O_QCL}). The regression analysis included all C_{N2O} in (a) but only those C_{N2O} measured at control sites (AN_0) in panel (c). The orthogonal regression analysis was repeated for standardised F_{N2O} with (b) showing all F_{N2O_GC} and F_{N2O_QCL}, and (d) depicting the orthogonal regression for AN_0 fluxes only. Ordinary least squares (dotted light grey line) resulted from the regression of Y on X; inverse least squares from the regression of X on Y (long dotted dark grey line). The major axis (black line) based on orthogonal regression of Y and X using a principal component analysis. Here, the squared residuals perpendicular to the line are minimised. Note, for the purpose of illustration axes in panel (c) and (d) have different scales. Table S4 in the supplements provides further results.

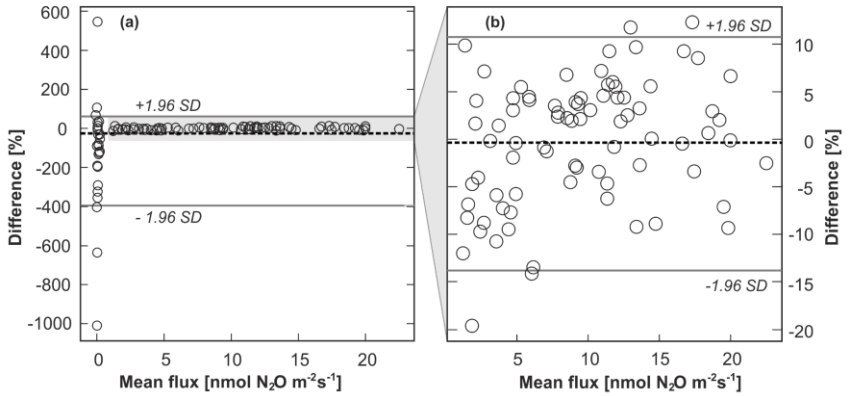

Figure 4: Bland Altman plots showing the difference between the GC and QCL method expressed as the percentage difference of the standard method A (F_{N2O_GC}) and the new method B (F_{N2O_QCL}) on the y-axis [((A-B)/mean)× 100] versus the mean of A and B on the x-axis. The limits of agreement are represented by continuous lines at ±1.96 standard deviation (SD) of the percentage difference. The inset (panel b) illustrates the same data but excludes F_{N2O_GC} and F_{N2O_QCL} from control (AN_0) sites. The percentage mean difference (bias) between F_{N2O_GC} and F_{N2O_QCL}, i.e. method A and B, is indicated by the gap between the dashed line (line of equality, which is not at zero) and an imaginary line parallel to the dashed line at y = 0. This figure is based on individual F_{N2O} (all treatment replicates). Results for mean F_{N2O} across replicates of the same treatment are provided in the supplements, see Table S5.

Deleted: of

Deleted: s

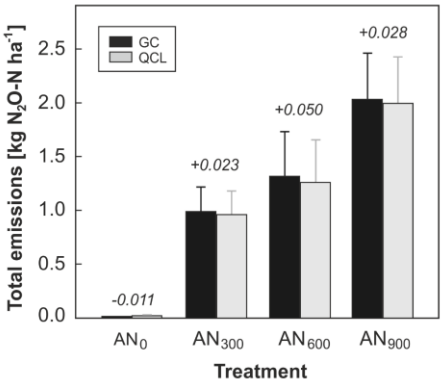

Figure 5: Cumulative N_2O emissions from each treatment (AN_{300}, AN_{600}, AN_{900}) and the control (AN_0) in kg N_2O-N ha^{-1} at the end of the campaign. Data are distinguished into GC (black bars) and QCL (grey bars) budgets. Error bars quantify the standard error of the mean (SEM). The absolute difference in kg N_2O-N ha^{-1} between the two budgets (GC-QCL) is highlighted by the number on the top of each bar-couple.

Deleted: of

Deleted: N_2O

Deleted: at

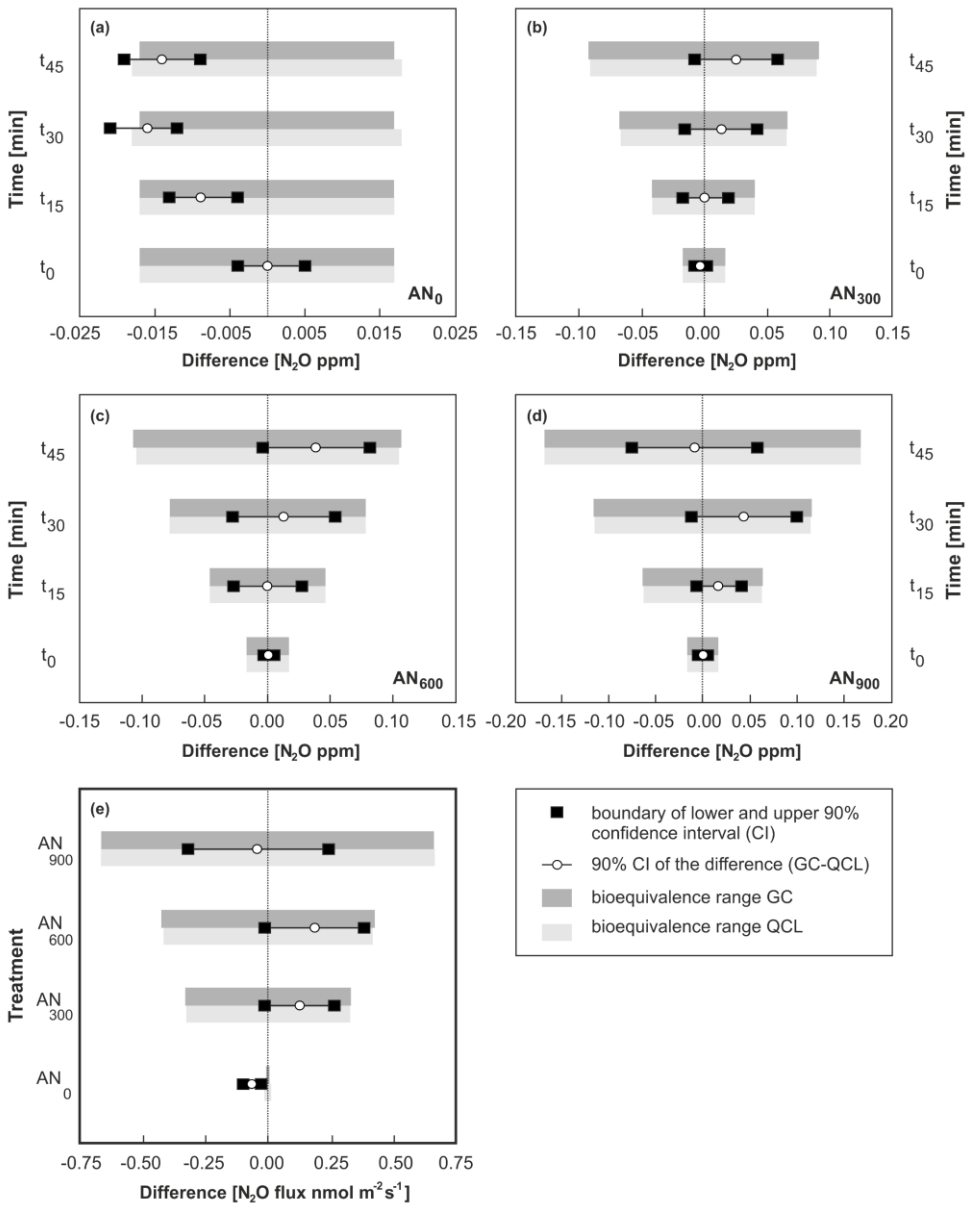
(a)
(b)
(c)
(d)
(e)
Time [min]
t45
t30
t15
t0
AN0
AN300
AN600
AN900
-0.025 -0.015 -0.005 0.005 0.015 0.025
-0.15 -0.10 -0.05 0.00 0.05 0.10 0.15
-0.20 -0.15 -0.10 -0.05 0.00 0.05 0.10 0.15 0.20
Difference [N2O ppm]
Treatment
AN 900
AN 600
AN 300
AN 0
-0.75 -0.50 -0.25 0.00 0.25 0.50 0.75
Difference [N2O flux nmol m-2 s-1]
boundary of lower and upper 90% confidence interval (CI)
90% CI of the difference (GC-QCL)
bioequivalence range GC
bioequivalence range QCL

Figure 6: Bioequivalence analysis for N_2O concentrations (C_{N2O}) in (a-d) and N_2O fluxes (F_{N2O}) in (e) with GC defined as the standard method. C_{N2O} and F_{N2O} based on QCL analysis were considered bioequivalent when the 90 % confidence interval (CI) of the difference between QCL and GC (x-axis) was completely within the predefined ± 5 % bioequivalence range of the difference of the standard method. The bioequivalence analysis was distinguished for C_{N2O} by sampling interval (t_0 ,t_{15} ,t_{30} , t_{45}) and treatment with panel (a) showing results for control sites (AN_0) and panels (b), (c) and (d) for AN_{300}, AN_{600} and AN_{900} treatment sites. Similarly, a bioequivalence analysis was conducted for F_{N2O} in panel (e) and distinguished by AN application rate on the y-axis.

Deleted: determined

Deleted: , here

Table 1: The GC and QCL methods in comparison: Details provided in the table relate to in this study and information provided were not generalised. NZD = New Zealand dollars.

	GC	QCL
Capital cost per device (NZD)	40,000	160,000
Labour effort for preparation and data processing of 100 samples (hours)	2 to 3	< 1
Transport of samples	required	not required
Storage of samples	required	optional
Analysis location	lab-based	field-based
Analysis time (days)	multiple days	immediate
Analysis cost per sample (NZD)	3.5	< 0.5
Possible injections (per hour)	7.5	~200
Lag time between injections (sec)	480	< 10
Injection procedure	manual/automated	manual
Injection of N_2O standards	required	required
Injection volume per sample (mL)	6	1
Carrier gas	N_2	N_2
Flow rate (L min^{-1})	0.4	1
Output of result data	post analysis	immediate

Deleted: Comparison of the

Deleted: injection

Deleted: .

Deleted: below

Deleted: specifically

Deleted: the application of the two techniques

Deleted: (i.e. have not been

Deleted:)

Supplementary material

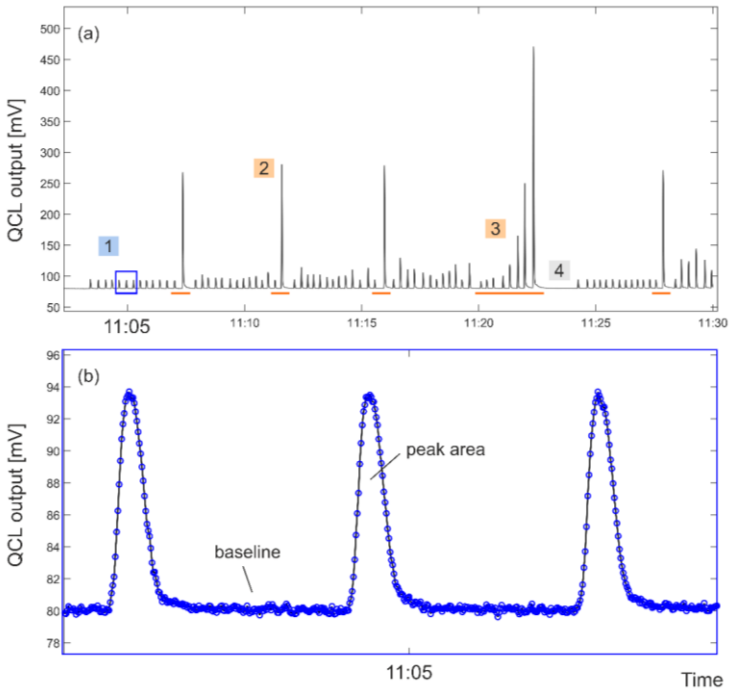

Figure S1: Example of QCL output data depicting how a one half-hourly peak progression sequence looked like. Panel (a) shows the full sequence for injected N_2O samples and standards in a given half-hour from 11-11:30 AM, 17 September 2020. Panel (b) captures three individual peaks from within this period (1) (blue rectangle). Single measurement points are depicted by blue dots with the black line showing an interpolated curvature. Orange bars underneath individual peaks in panel (a) distinguish injected N_2O standards from N_2O samples. (2) identifies 1 ppm and 5 ppm standards injected after every 12 samples, here serving as a running control; (3) shows an example of an injected standard line of known N_2O concentration (range: 0.2–10 ppm); and (4) the lag time that was required to ensure sufficient flushing of the QCL sample cell after injecting a sample or standard (here 10 ppm) of higher N_2O concentration.

Deleted: half

Deleted: time

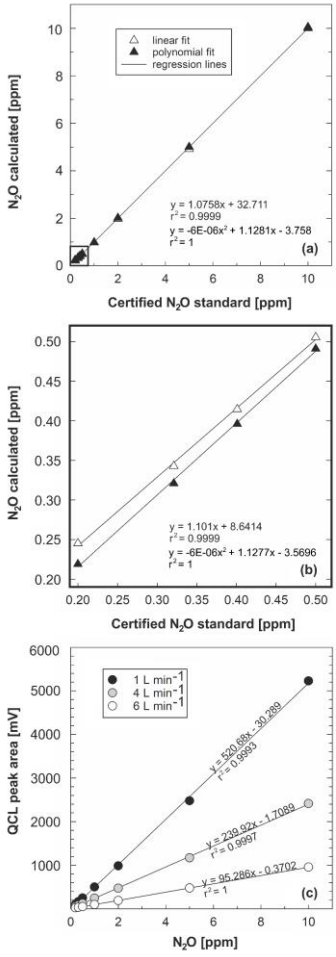

Figure S2: Tests conducted prior to the main study showing the calculated normal linear relationship between output peak area and N_2O concentration (C_{N2O}) for different scenarios and ranges of N_2O standards injected: (a) from 0.2 to 10 ppm, and (b) from 0.2 to 0.5 ppm, (c) demonstrates the effect of flow rate in L min^{-1} on the slope of the associated regression lines, output peak area and measured N_2O concentration in ppm.

Deleted: for different ranges of N_2O standards

Deleted: ;

Table S1: Chronology of experimental activities.

Date	Activity
15-Aug-19	Trial site fenced off
	Preliminary injection into QCL: testing different syringe types
20-Aug-19	Installation of chamber collars
30-Aug-19	Preliminary injections into QCL: testing different flow rates
10-Sep-19	Treatment application to chamber and soil plots
	Gas and soil sampling – run 1
11-Sep-19	Gas and soil sampling – run 2
12-Sep-19	Gas and soil sampling – run 3 & 4
13-Sep-19	Gas and soil sampling – run 5
14-Sep-19	Gas and soil sampling – run 6
15-Sep-19	Gas and soil sampling – run 7 & 8
16-Sep-19	Gas and soil sampling – run 9
17-Sep-19	Sample injection into QCL

Table S2: Certified N_2O standards used in this study and associated uncertainty levels. Standards printed in bolt fond were used in quadratic curve models to calculate final N_2O concentration of the samples taken from static chambers.

N_2O [µL L^{-1}] [ppmv]	**Uncertainty** [alpha/beta] [%]	**Background** (gas)	**Company** (name)
0.200	± 0.01	Nitrogen	BOC Ltd.
0.321	± 0.1–0.9%	Cryogenic UltraPure Air	Praxair, Inc.
0.3252	± 0.01	Air	NIWA
0.401	± 0.1–0.9%	Cryogenic UltraPure Air	Praxair, Inc.
0.500	± 0.01	Nitrogen	BOC Ltd.
1.00	± 0.01	Nitrogen	BOC Ltd.
2.00	± 0.02	Nitrogen	BOC Ltd.
5.00	± 0.1	Nitrogen	BOC Ltd.
10.00	± 0.2	Nitrogen	BOC Ltd.
20.00	± 0.2	Nitrogen	BOC Ltd.
50.00	± 1.0	Nitrogen	BOC Ltd.
100.00	± 1.0	Nitrogen	BOC Ltd.

Deleted: and

Deleted: Certified N_2O s

Deleted: concentrations

Deleted: sample

Formatted: Font: Not Bold

Table S3: This table presents the measured values of nitrous oxide fluxes (F_{N2O}) analysed by GC and QCL, soil water-filled pore space (WFPS), soil ammonium (NH_4^+) and nitrate (NO_3^-) content of the control (AN_0) and across the different treatments of ammonium-nitrate (AN_{300}, AN_{600}, AN_{900}). The associated standard error of the mean (SEM) is provided at the right-hand side of each control/treatment column.

Deleted: applied

Deleted: right

date	AN_0	SEM	AN_{300}	SEM	AN_{600}	SEM	AN_{900}	SEM
GC nitrous oxide flux [F_{N2O_GC} in nmol N_2O m^{-2} s^{-1}]								
10-Sep-2019	0.04	0.05	3.56	1.20	1.95	0.19	2.49	0.52
11-Sep-2019	0.13	0.04	9.93	1.97	9.63	3.44	14.88	3.55
12-Sep-2019*	0.06	0.05	8.67	1.73	8.02	2.92	15.87	3.96
12-Sep-2019*	0.06	0.01	8.42	2.62	8.19	3.23	14.87	3.15
13-Sep-2019	-0.05	0.03	6.43	3.00	11.57	3.68	15.16	3.76
14-Sep-2019	0.03	0.01	7.46	2.19	10.71	3.43	16.71	2.46
15-Sep-2019*	0.02	0.03	5.03	0.80	10.21	2.84	14.85	3.58
15-Sep-2019*	0.03	0.03	6.92	1.57	9.98	2.96	13.88	2.75
16-Sep-2019	0.02	0.04	3.06	1.33	6.37	2.45	10.29	1.67
QCL nitrous oxide flux [F_{N2O_QCL} in nmol N_2O m^{-2} s^{-1}]								
10-Sep-2019	0.00	0.03	3.65	1.18	2.17	0.19	2.74	0.60
11-Sep-2019	0.21	0.05	9.40	1.83	8.88	3.14	13.57	3.04
12-Sep-2019*	0.14	0.07	8.19	1.60	7.94	2.92	15.17	3.71
12-Sep-2019*	0.06	0.02	8.02	2.47	8.04	3.11	15.46	3.57
13-Sep-2019	0.09	0.08	6.25	2.77	10.91	3.33	15.09	4.05
14-Sep-2019	0.03	0.02	7.30	2.10	10.66	3.24	17.22	2.71
15-Sep-2019*	0.17	0.01	5.30	0.86	9.46	2.42	14.81	3.65
15-Sep-2019*	0.18	0.03	6.95	1.33	10.27	2.89	14.36	2.69
16-Sep-2019	0.06	0.01	3.28	1.63	6.63	2.51	10.97	1.99
Water filled pore space of the soil [%]								
10-Sep-2019	79.43	0.48	78.66	1.82	78.06	1.40	82.30	2.35
11-Sep-2019	81.64	0.59	84.97	1.68	80.16	0.53	82.13	1.79
12-Sep-2019	82.18	1.12	80.63	1.23	79.35	1.05	79.20	1.00
13-Sep-2019	79.62	0.95	79.72	1.87	76.62	2.08	78.13	1.76
14-Sep-2019	79.43	0.56	80.60	2.00	78.37	1.74	77.78	1.19
15-Sep-2019	79.79	0.50	81.70	2.65	77.17	1.49	76.81	0.37
16-Sep-2019	77.92	1.06	81.05	1.98	73.93	1.60	77.41	1.80
Soil ammonium [kg NH_4^+ ha^{-1}]								
10-Sep-2019	1.82	0.50	81.73	5.20	89.36	2.72	264.63	17.19
11-Sep-2019	0.81	0.11	52.26	7.18	141.51	11.08	233.63	33.62
12-Sep-2019	2.15	0.57	44.61	6.52	109.37	6.77	213.76	3.41
13-Sep-2019	2.21	0.33	36.88	6.75	124.48	9.36	194.76	18.88
14-Sep-2019	3.71	0.09	20.31	5.07	59.88	6.05	188.70	18.05
15-Sep-2019	1.84	0.64	9.58	0.99	78.98	12.30	155.84	18.49
16-Sep-2019	1.80	0.29	13.21	3.23	38.50	4.59	124.38	7.64

	Soil nitrate [kg NO_3^- ha^{-1}]							
10-Sep-2019	2.99	0.37	83.67	3.87	104.95	1.33	267.77	15.17
11-Sep-2019	2.46	0.18	69.08	6.54	149.95	8.62	248.89	33.69
12-Sep-2019	2.29	0.07	79.41	6.57	142.52	8.61	230.94	7.36
13-Sep-2019	1.64	0.20	82.21	7.92	149.85	6.25	232.40	13.77
14-Sep-2019	1.84	0.35	73.37	12.71	114.20	8.41	237.77	8.96
15-Sep-2019	2.47	0.31	78.91	1.51	162.60	8.72	231.51	16.94
16-Sep-2019	1.85	0.22	92.49	16.22	134.38	7.60	211.88	18.92

* flux measurements conducted twice daily at 10 AM and 12 PM
SEM = standard error of the mean

Table S4: Results from the linear functional relationship analysis (orthogonal regression). Columns labelled C_{N2O} show the results of the regression analysis when using standardised N_2O concentrations. Columns labelled F_{N2O} provide results based on standardised N_2O fluxes. Part of the regression analysis was to characterise both data streams by treatment and control, i.e. first including all data (AN_0, AN_{300}, AN_{600}, AN_{900}) in the analysis and then, separately, only the control (AN_0).

	C_{N2O} all AN	**C_{N2O}** AN_0 only	**F_{N2O}** all AN	**F_{N2O}** AN_0 only
Number of observations	432	108	108	27
Response mean	-0.003164	0.3272	-0.004008	0.3776
Explanatory mean	0.003164	-0.3272	0.004008	-0.3776
Response variance	0.9811	1.238	0.9860	1.139
Explanatory variance	1.021	0.5551	1.023	0.6029
r^2 value	0.9928	0.1753	0.9922	0.0939
r value	0.9964	0.4187	0.9961	0.3064
Angle between Y on X and X on Y	0.2068	42.32	0.2229	54.59
Major eigenvalue	1.999	1.384	2.005	1.241
Minor eigenvalue	0.003606	0.4096	0.003901	0.5017
Bootstrap resampling	200	200	200	200
Ordinary least squares:				
Constant	-0.006253	0.532	-0.007926	0.537
Standard error	0.003914	0.1038	0.007861	0.26
Lower	-0.01331	0.3101	-0.02204	-0.02
Upper	0.001710	0.734	0.006998	1.030
Slope	0.9766	0.625	0.9778	0.421
Inverse least squares:				
Constant	-0.006276	1.49	-0.007957	2.072
Standard error	0.003902	0.6585	0.007902	82.46
Lower	-0.01369	0.9211	-0.02246	-44.95
Upper	0.001786	3.478	0.007118	18.732
Slope	0.9837	3.567	0.9854	4.486
Major axis:				
Constant	-0.006264	1.108	-0.007941	1.326
Standard error	0.003904	0.44	0.007872	40.17
Lower	-0.01349	0.7105	-0.02217	-19.84
Upper	0.001610	2.484	0.006920	9.937
Slope	0.9801	2.387	0.9815	2.511

Table S5: Bland-Altman analysis for F_{N2O_GC} and F_{N2O_QCL} distinguished by treatment in units nmol m^{-2} s^{-1}, if not specified otherwise. This table provides a summary based on mean F_{N2O_GC} and F_{N2O_QCL} across replicates of the same treatment. Fig. 4, instead, illustrates the results of individual F_{N2O_GC} and F_{N2O_QCL} (not depicted in the below table) for each replicate and each treatment as the percentage mean difference between the two methods, i.e. GC (A) and QCL (B).

Sampling	**Treatment**	**GC (A)**	**QCL (B)**	**Mean**	**Difference**	**Difference (%)**
[No.]	[kg N ha^{-1}]	F_{N2O_GC}	F_{N2O_QCL}	(A+B)/2	(A-B)	((A-B)/mean)*100
1	0	0.04	0.00	0.02	0.04	182.48
1	300	3.56	3.65	3.61	-0.09	-2.59
1	600	1.95	2.17	2.06	-0.23	-11.11
1	900	2.49	2.74	2.61	-0.24	-9.24
2	0	0.13	0.21	0.17	-0.08	-44.70
2	300	9.93	9.40	9.67	0.53	5.51
2	600	9.63	8.88	9.26	0.75	8.11
2	900	14.88	13.57	14.22	1.31	9.20
3	0	0.06	0.14	0.10	-0.08	-78.52
3	300	8.67	8.19	8.43	0.48	5.69
3	600	8.02	7.94	7.98	0.08	0.98
3	900	15.87	15.17	15.52	0.70	4.51
4	0	0.06	0.06	0.06	0.00	1.93
4	300	8.42	8.02	8.22	0.39	4.79
4	600	8.19	8.04	8.11	0.15	1.82
4	900	14.87	15.46	15.16	-0.59	-3.89
5	0	-0.05	0.09	0.02	-0.14	-595.36
5	300	6.43	6.25	6.34	0.18	2.88
5	600	11.57	10.91	11.24	0.66	5.88
5	900	15.16	15.09	15.13	0.07	0.49
6	0	0.03	0.03	0.03	0.00	4.14
6	300	7.46	7.30	7.38	0.16	2.19
6	600	10.71	10.66	10.68	0.05	0.47
6	900	16.71	17.22	16.96	-0.51	-3.02
7	0	0.02	0.17	0.09	-0.15	-157.04
7	300	5.03	5.30	5.17	-0.27	-5.22
7	600	10.21	9.46	9.84	0.75	7.67
7	900	14.85	14.81	14.83	0.03	0.22
8	0	0.03	0.18	0.10	-0.15	-149.70
8	300	6.92	6.95	6.94	-0.02	-0.34
8	600	9.98	10.27	10.13	-0.29	-2.86
8	900	13.88	14.36	14.12	-0.48	-3.39
9	0	0.02	0.06	0.04	-0.04	-105.26
9	300	3.06	3.28	3.17	-0.22	-6.86
9	600	6.37	6.63	6.50	-0.26	-4.02
9	900	10.29	10.97	10.63	-0.68	-6.39

Table S6: Bioequivalence analysis for N_2O concentrations (C_{N2O}) and associated fluxes (F_{N2O} in bottom panel of the table). C_{N2O_QCL} and F_{N2O_QCL} were considered bioequivalent when the 90% confidence interval of the difference was completely within the predefined ±5% bioequivalence range of difference to C_{N2O_GC} and F_{N2O_GC} (corresponding to a test with size 0.05). rep. = replicates, d.f = degrees of freedom, s.e.d = standard error of the difference, LSD = least significant difference

Time/ Treatment	**Mean**		**Standard error of the difference of the mean**			**LSD**	**90% confidence interval**			**Bioequivalence range**			
AN_0	**C_{N2O_GC}** [ppm]	**C_{N2O_QCL}** [ppm]	rep.	d.f	s.e.d	s.e.d	difference (GC-QCL)	lower	upper	GC lower	GC upper	QCL lower	QCL upper
t_0	0.333	0.332	27	26	0.0027	0.0046	0.000	-0.004	0.005	-0.017	0.017	-0.017	0.017
t_{15}	0.333	0.342	27	26	0.0028	0.0048	-0.009	-0.013	-0.004	-0.017	0.017	-0.017	0.017
t_{30}	0.335	0.352	27	26	0.0029	0.0049	-0.016	-0.021	-0.012	-0.017	0.017	-0.018	0.018
t_{45}	0.340	0.354	27	26	0.0027	0.0046	-0.014	-0.019	-0.009	-0.017	0.017	-0.018	0.018
AN_{300}													
t_0	0.333	0.336	27	26	0.0028	0.0048	-0.003	-0.007	0.002	-0.017	0.017	-0.017	0.017
t_{15}	0.822	0.821	27	26	0.1090	0.0186	0.001	-0.017	0.020	-0.041	0.041	-0.041	0.041
t_{30}	1.341	1.327	27	26	0.0168	0.0286	0.014	-0.015	0.042	-0.067	0.067	-0.066	0.066
t_{45}	1.831	1.804	27	26	0.0192	0.0327	0.026	-0.007	0.059	-0.092	0.092	-0.090	0.090
AN_{600}													
t_0	0.336	0.335	27	26	0.0023	0.0042	0.001	-0.003	0.005	-0.017	0.017	-0.017	0.017
t_{15}	0.912	0.912	27	26	0.0160	0.0273	0.000	-0.027	0.027	-0.046	0.046	-0.046	0.046
t_{30}	1.563	1.550	27	26	0.0242	0.0412	0.013	-0.028	0.054	-0.078	0.078	-0.078	0.078
t_{45}	2.143	2.104	27	26	0.0250	0.0427	0.039	-0.004	0.082	-0.107	0.107	-0.105	0.105
AN_{900}													
t_0	0.338	0.337	27	26	0.0028	0.0319	0.001	-0.004	0.005	-0.017	0.017	-0.017	0.017
t_{15}	1.285	1.268	27	26	0.0136	0.1380	0.017	-0.006	0.041	-0.064	0.064	-0.063	0.063
t_{30}	2.338	2.294	27	26	0.0325	0.1959	0.044	-0.012	0.100	-0.117	0.117	-0.115	0.115
t_{45}	3.370	3.379	27	26	0.3900	0.2850	-0.009	-0.076	0.058	-0.169	0.169	-0.169	0.169
Treatment	**F_{N2O_GC}** [nmol N_2O m^{-2} s^{-1}]	**F_{N2O_QCL}**											
AN_0	0.0387	0.1048	27	26	0.0187	0.0319	-0.066	-0.098	-0.034	-0.002	0.002	-0.005	0.005
AN_{300}	6.610	6.483	27	26	0.0809	0.1380	0.127	-0.011	0.265	-0.331	0.331	-0.324	0.324
AN_{600}	8.514	8.329	27	26	0.1149	0.1959	0.185	-0.011	0.381	-0.426	0.426	-0.416	0.416
AN_{900}	13.222	13.265	27	26	0.1671	0.2850	-0.043	-0.328	0.242	-0.661	0.661	-0.663	0.663

Formatted: Font: 10 pt